LAWRENCE
LIVERMORE
NATIONAL
LABORATORY

LLNL-JRNL-807185

Holocene paleoclimate change in the western U.S.: The importance of chronology in discerning patterns and drivers

S. R. H. Zimmerman, D. B. Wahl

March 13, 2020

Quaternary Science Reviews

Disclaimer

Holocene paleoclimate change in the western US: The importance of chronology in discerning patterns and drivers

Susan R.H. Zimmerman [a, *], David B. Wahl [b, c]

[a] Center for Accelerator Mass Spectrometry, Lawrence Livermore National Lab, Livermore, CA, 94550, USA
[b] U.S. Geological Survey, 345 Middlefield Rd. MS-975, Menlo Park, CA, 94025, USA
[c] Department of Geography, University of California, Berkeley, CA, 94720, USA

A B S T R A C T

Sediment in lakes and meadows forms a powerful archive that can be used to reconstruct environmental change through time. Reconstructions of lake level, of chemical, biological, and hydrological conditions, and of surrounding vegetation provide detailed information about past climate conditions, both locally and regionally. Indeed, most of our current knowledge of centennial- to millennial-scale climate variability in the arid western United States, where information about past hydroclimate is particularly important, comes from such sediment-based reconstructions. The pressing need for robust, precise predictions of future conditions is a significant motivation for paleoclimate science, and current research questions frequently require Holocene reconstructions to be resolved at sub-centennial timescales. Increasingly, regional syntheses seek to identify synoptic-scale patterns similar to those defined from modern observations (seasonal, interannual, multi-decadal, etc.) or to compare with the output of climate model simulations. However, the age control on existing records, especially those more than about 20 years old, is often sufficient only for millennial-scale interpretation. Here we assess the age control for 84 published and unpublished records from lakes and meadows in the Great Basin, California, and desert southwest, and use Bayesian modeling to evaluate the 95% uncertainty ranges for the 42 best-dated records. In the Late Holocene, about half of the 42 records have <400-year mean uncertainty ranges; however, high-precision age control is especially critical for young records, used to develop an accurate understanding of a proxy's response to known climate variations. In the Middle Holocene, records vary from 400 to >800-year mean uncertainty and records of the Early Holocene have 600- to >1400-year mean uncertainty ranges. We find that the largest control on modeled uncertainties is dating density, with at least 2 dates/kyr being optimal and suggest obtaining "range-finder" dates at the onset of a study to better predict the total number of dates needed for an adequate age model. Such a density avoids a commonly observed phenomenon of significant peaks in uncertainty arising in gaps between age control points. Analysis of the uncertainties associated with proxy shifts reveal that more than half are >400 years. Although such large uncertainties currently prevent sub-centennial interpretations in most cases, increased dating density, strategic use of limited funds (including budgeting for a 2 date/kyr minimum at the proposal stage), construction of age-depth models with Bayesian methods, and critical evaluation of chronological uncertainty will shed light on past climate variability at finer timescales, enhancing our understanding of global and regional drivers of western U.S. climate.

* Corresponding author.
E-mail addresses: zimmerman17@llnl.gov (S.R.H. Zimmerman), dwahl@usgs.gov (D.B. Wahl).

1. Introduction

In order to better understand drivers and impacts of changes in the pre-industrial global climate system, the paleoclimate community is increasingly making an effort to synthesize the results of extant climate reconstructions, both as formal synthesis papers and through correlation of new records. Studies often compile decades of paleoclimate data from a variety of archives and across broad geographic regions, looking for spatial patterns (e.g., Mensing et al., 2013; Metcalfe et al., 2015; Hermann et al., 2018). Syntheses and many individual studies also frequently make correlations to

canonical records interpreted to record large-scale changes, such as in the North Atlantic (Dansgaard et al., 1993; Grootes and Stuiver, 1997), the tropics (Haug et al., 2001) or a monsoon system (Wang et al., 2001) in order to identify global teleconnections in the climate system. Further, several syntheses have aimed to compare compiled paleoclimate datasets with the simulations of various regions and time-slices from global climate models (Kohfeld and Harrison, 2000; Harrison et al., 2003; Bartlein et al., 2010).

The degree of success in discerning patterns of change is largely determined by the ability to accurately and precisely correlate between paleorecords. These correlations, in turn, depend on the quality and quantity of the age control points and the method used to construct age-depth models for all the records involved. In general, when several records are correlated the uncertainties in underlying age models are ignored, perhaps assuming that they are small relative to the scatter of the paleoclimate signals. As a result, changes observed in proxy data from multiple records may appear to have a temporal relationship, when in fact they may be separated by several centuries or more, thus making inferences about drivers of change tenuous. A recent exception is the synthesis of Rodysill et al. (2018), which applied clear minimum age control standards in order for a study to be considered, and then incorporated uncertainties from newly constructed Bayesian models into the analysis of climate patterns. Here we focus on assessing age control and construction of age models for western U.S. records, as a prelude to examination of paleoclimatic implications.

For Holocene terrestrial records, radiocarbon dates are generally the most common, with U-series dating applied to speleothems (Oster et al., 2009; Steponaitis et al., 2015), $^{40}Ar/^{39}Ar$ dating (Chen et al., 1996; Kent et al., 2002) and tephrochronology (Sarna-Wojcicki et al., 1991; Negrini et al., 2000) to volcanic tephras, luminescence methods to fluvial deposits and landforms (Owen et al., 2007; Rhodes, 2011) and cosmogenic-nuclide dating to glacial, fluvial and alluvial landforms (Rood et al., 2011; Antinao et al., 2016). Each method has strengths and weaknesses, and it is critical to assess the quality of the underlying age models when comparing proxy data between sites.

In this review we are concerned with assessing the timing of changes in terrestrial conditions in the western U.S. over the past 12,000 years. Since high-resolution proxy data describe change more or less continually (as opposed to snapshots from geomorphic features) and stratigraphic continuity can bolster the interpretation of ages between dates, sediment cores are the primary focus of this paper. We thus review all the available Holocene climate reconstructions from lakes and meadows in California, the Great Basin, and the desert southwest. Many of these records have been used as targets for correlation several times since their original publication, but with little attention to the precision and accuracy of their age models. Using all the available information about core stratigraphy and age control, we assess the uncertainties associated with the age models. Our goals are to identify sites with age information that will support decadal-to centennial-scale interpretation of paleoclimatic proxies, to distinguish the factors involved in a quality age model, and to suggest some best practices for building or revising chronologies for paleorecords.

The sites discussed here (Fig. 1, Table 1) are affected by changes in precipitation delivered from the Pacific, in the form of large high-latitude winter-season frontal systems, sub-tropical moisture from atmospheric river storms, and/or sub-tropical moisture delivered as summer precipitation from the North American monsoon (though some monsoon moisture originates in the Gulf of Mexico). Changes in the large-scale ocean-atmosphere system that drive these various types of storms are indicated on various timescales by canonical records of the North Atlantic and tropics. During the glacial and deglacial periods, climatic shifts often drove changes in temperature that were recorded in the Greenland ice cores, while through the Holocene paleoclimate archives from the tropics and sub-tropics have recorded shifting insolation, strengthening and weakening of the monsoons, and the onset and development of the El Niño-Southern Oscillation (ENSO) system. To place changes in western US records within this framework, we use the Greenland GISP2 oxygen-isotope record (Grootes and Stuiver, 1997; Stuiver and Grootes, 2000) and the Cariaco Basin % Ti record of the position of the Intertropical Convergence Zone (Haug et al., 2001) (ITCZ, Fig. 2). We note that each of these records has its own chronological uncertainties, but do not deal with those uncertainties in this review.

Several periods during the Holocene stand out as times of widespread, potentially abrupt change (Fig. 2). These periods are characterized by different durations; some are quite abrupt (years to decades), and others appear to be shifts over a longer period (centennial or multi-centennial). Likewise, the age of the changes is known quite precisely for some and very poorly for others, and these two characteristics may not be unrelated. The periods of interest and the studies that help define them are:

i) the end of the Younger Dryas (YD) period at 11,650 ± 99 cal yr BP (Walker et al., 2009), an abrupt change in conditions in the North Atlantic (Alley, 2000) shown to have widespread repercussions in the northern hemisphere (Haug et al., 2001; Wang et al., 2001; Polyak et al., 2004);
ii) the organization of the modern North American monsoon (NAM) system between about 8000 and 7500 years ago, suggested by records of ocean-atmosphere circulation from the Gulf of California region (Barron et al., 2012), and with implications particularly for records on the modern boundaries of the core monsoon region (Bacon et al., 2006; Kirby et al., 2015);
iii) the onset of the Neoglacial period, often cited as about 4000 years ago but poorly defined, when glaciers in the northern hemisphere mountains reformed or advanced (Owen et al., 2003; Davis et al., 2009; Bowerman and Clark, 2011), and possibly correlative to increasing wetness at lower elevation or lower latitude sites (Stine, 1990; Bacon et al., 2006; Kirby et al., 2015; Adams and Rhodes, 2019);
iv) extreme aridity starting about 2800 years ago and lasting around 1000 years, as noted by Mensing et al. (2013) at a number of western U.S. sites and termed the Late Holocene Dry Period (LHDP);
v) the shift from the warm dry conditions of the Medieval Climate Anomaly (MCA) to the cold wet conditions of the Little Ice Age (LIA), about 500 years ago (Stine, 1994; Haug et al., 2001; Heusser et al., 2015).

Each of these climate shifts has been described from multiple locations, in some cases at very high proxy-sampling resolution and temporal precision, and in other cases at much lower resolution and precision. Each is associated with a physical mechanism that suggests an impact on western US climate or with significant evidence of regional change (or both), and each has become a paradigm in the literature, a focus of correlation for newer records covering the relevant time period and/or aspect of the climate system. However, in order to examine patterns for the region as a whole and their relationship to the global climate framework, the question of age control is paramount.

2. Dating methods

To understand the spatial extent of climatic and other

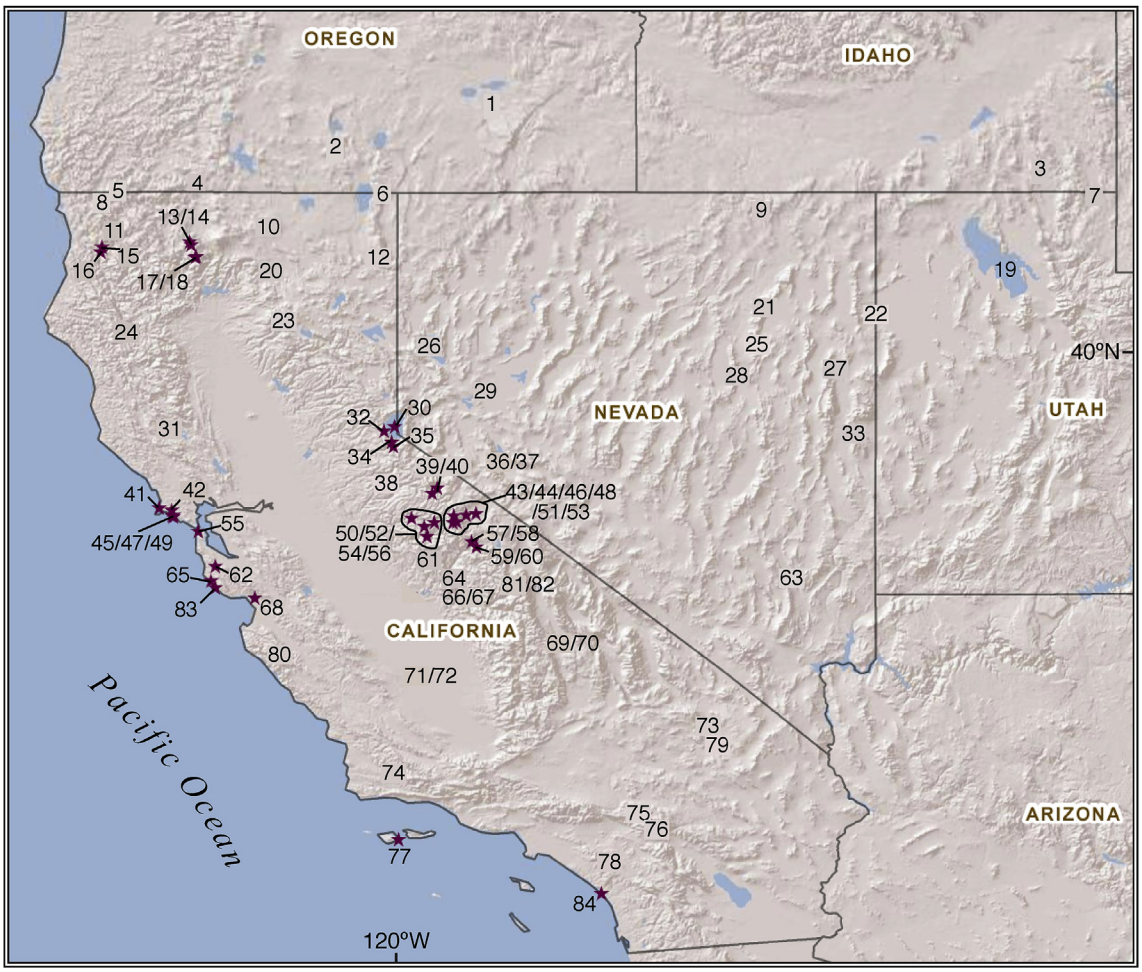

Fig. 1. Map of the western United States showing the locations of studies used in this review. Sites are indicated by numbers: see Table 1 for site name and locality information.

environmental events evident in paleo records, and whether they were synchronous, sequential, or randomly ordered, it is critically important to collect as much age information as possible for a record, and also *to assess both the analytical and geological uncertainties* associated with the available age control. Analytical uncertainties are those associated with the measurement of isotopic ratios or a luminescence signal, counting of historical pollen, or other laboratory analysis. They include considerations such as sample handling, machine conditions, expertise of the observer (for pollen or varve studies), measurement of standard reference materials (including blanks), and conversion of measured quantities to age. Geological uncertainties stem from suitability of the material for the intended chronological analysis, the processes involved in deposition of archive materials (including pre-aging and/or redeposition of material prior to being incorporated in the sediment matrix, recycling of crystals in a magma chamber, etc.), the relationship between the formation and deposition of dated material and the event of interest, the degree and type of alteration of the dated material, and artifacts of coring and sampling processes.

Although radiocarbon analysis is the most common technique used to date organic material from the last ~40,000 years in sedimentary sequences, multiple chronometers are frequently used together to date a single sediment sequence. In the western US and other tectonically active areas, material ejected during volcanic eruptions, known collectively as tephra, can be an important source of chronological control. In some sites, exotic pollen such as corn (*Zea mays),* storksbill filaree (*Erodium cicutarium*), or eucalyptus (*Eucalyptus* spp*)* can be used as age control for records preserving the historical period, if the time of introduction is well known. Additionally, the relatively short-lived radiogenic isotopes ^{210}Pb and ^{137}Cs, the latter of which was produced in the atmosphere by nuclear-weapons testing, are frequently used to provide age control for sediment deposited within the last century. Although each technique has strengths and weaknesses, the fundamental concern is the same: identifying assumptions and sources of uncertainty, both analytical and geological, so that the total uncertainty of an age model can be expressed accurately. We summarize the considerations relating to the main techniques used for dating of Holocene sequences below.

2.1. Radiocarbon dating

In general, chronologies for both terrestrial and marine records of the post-glacial period have been constructed by measuring the radiocarbon content of carbon-based materials such as wood, charcoal, plant material, shells, or bulk sediment. Radiocarbon is made in the atmosphere by the interaction of high-energy particles from cosmic-ray cascades with ^{14}N in a^{14}N (n,p) ^{14}C reaction. The production rate of ^{14}C is variable, depending on the same factors as other cosmogenic nuclides made in the atmosphere (e.g., meteoric ^{10}Be): the flux of cosmogenic rays from space and shielding of Earth's atmosphere by the geomagnetic field (which varies with

Table 1
Site information for all records considered in the current review.

Site #	Site Name	State	Latitude (°N)	Longitude (°W)	Elevation (m)	Year of core	Year of pub	Min age	Max age	Discussed in Section	References
1	Diamond Pond	OR	43.1040	−118.8160	1265	1978	1987	−28	6850	4.2	Wigand (1987); Foit and Mehringer (2016)
2	Deadhorse Lake	OR	42.5606	−120.7781	2248	<2007	2007	−49	13,950	4.1	Minckley et al. (2007)
3	Swan Lake	ID	42.2940	−111.9917	1453	1962	1966	0	14,000	4.2	Bright (1966)
4	Hobart Lake	OR	42.0980	−122.4810	1458	2011	2015	pres	7930	5	White et al. (2015)
5	Bolan Lake	OR	42.0222	−123.4591	1638	1999	2005	−48	14,500	5	Briles et al. (2008), Briles et al. (2005), Briles (2008)
6	Lily Lake	CA	41.9758	−120.2097	2042	<2007	2007	pres	10,000	4.1	Minckley et al. (2007)
7	Bear Lake	UT/ ID	41.9540	−111.3170	1805	1996	2009	pres	>12,000	5	Moser and Kimball, 2009; Colman et al. (2009)
8	Sanger Lake	CA	41.9017	−123.6469	1550	2003	2008	−53	14,200	5	Briles et al. (2008)
9	Mission Cross Bog	NV	41.7856	−115.4839	2424	1997, 2005	2008	−47	4930	5	Mensing (2008), Allan (2003); Norman (2007)
10	Medicine Lake	CA	41.5831	−121.6031	2036	2000	2003	−50	11,400	4.1	Starratt et al. (2003), Starratt (2009)
11	Ogaromtoc Lake	CA	41.4860	−123.5410	596	2009	2015	−59	3340	5	Crawford et al. (2015)
12	Patterson Lake	CA	41.3821	−120.2203	2743	<2007	2007	pres	12,200	5	Minckley et al. (2007)
13	Crater Lake	CA	41.3831	−122.5792	2288	1996	2000	0	8125	4.1	Mohr et al. (2000)
14	Bluff Lake	CA	41.3465	−122.5599	1921	1995	2000	0	13,470	5	Mohr et al. (2000)
15	Twin Lake, CA	CA	41.3230	−123.6688	1200	2001	2002	pres	22,850	5	Wanket (2002)
16	Fish Lake	CA	41.2630	−123.6830	541	2008	2015	−58	2850	5	Crawford et al. (2015)
17	Cedar Lake	CA	41.2072	−122.4971	1743	1989	1989	pres	12,000	4.2	West (1989), Whitlock et al. (2008)
18	Mumbo Lake	CA	41.1910	−122.5100	1860	2005	2005	25	15,125	5	Daniels et al. (2005)
19	Great Salt Lake	UT	41.0170	−112.4670	1280	1996	2013	−46	39,900	5	Thompson et al. (2016)
20	Flycatcher Basin	CA	41.0146	−121.5721	924	1992	2008	−42	8220	4.2	Anderson et al. (2008)
21	Favre Lake	NV	40.5736	−115.3966	2899	2008	2015	−58	7625	5	Wahl et al. (2015)
22	Blue Lake Marsh	UT	40.5000	−114.0360	1297	2004	2009	1000	15,000	5	Louderback and Rhode (2009)
23	Little Willow Lake	CA	40.4110	−121.3895	1829	2003	2003	pres	16,155	4.2	West (2004)
24	SchellingsBogSB70	CA	40.2777	−123.3591	910	1970	2004	−20	4500	4.2	Barron et al. (2004)
25	Ruby Lake/Marsh	NV	40.1100	−115.5100	1818	<1992	1992	−50	41,075	4.1	Thompson (1992)
26	Pyramid Lake	NV	40.0720	−119.5835	1156	1997, 1998	2002	−50	7630	4.1, 4.3	Benson et al. (2002), Mensing et al. (2004)
27	Stonehouse Meadow	NV	39.7856	−114.5428	1740	2010	2013	−60	8080	5	Mensing et al. (2013), Tunno and Mensing (2017)
28	Newark Valley Pond	NV	39.7369	−115.7485	1750	2001	2008	−51	5530	5	Mensing et al. (2006), Mensing (2008)
29	Big Soda Lake	NV	39.5253	−118.8780	1216	2010	2013	−59	1600	5	Reidy (2013)
30	Lake Tahoe	CA	39.0900	−120.0300	1900	1999	2008	−49	7015	4.1	Osleger et al. (2008)
31	Clear Lake	CA	39.0650	−122.8400	404	1973	1981	−23	>14,000	4.2	Adam et al. (1981), Adam (1988)
32	Lily Pond	CA	39.0347	−120.1625	2010	2001	2009	−51	14,000	5	Beaty and Taylor (2009)
33	Stella Lake	NV	39.0054	−114.3190	3170	2007	2009	−57	6810	5	Reinemann et al. (2009)
34	Fallen Leaf	CA	38.8975	−120.0631	1942	2010	2016	−60	14,000	5	Noble et al. (2016), Ball et al. (2019)
35	Osgood Swamp	CA	38.8460	−120.0416	1996	<1967	1967			4.1	Adam (1967)
36	Walker Lake	NV	38.6668	−118.7421	1196	1984	1991	−34	6100	4.2, 4.3	Benson et al. (1991), Bradbury et al. (1989)
37	Walker Lake	NV	38.6668	−118.7421	1196	2000	2004	−50	2700	5	Yuan et al. (2006a, 2006b); Yuan et al. (2004)
38	Lake Moran	CA	38.3829	−120.1304	2030	1988	1990	−38	17,900	4.2	Edlund and Byrne (1991)
39	Kirman Lake	CA	38.3402	−119.4995	2174	2000	2016	−50	9220	5	MacDonald et al. (2016)
40	Hidden Lake	CA	38.2613	−119.5365	2379	2002	2006	−52	15,000	5	Potito et al. (2006)
41	Creamery Bay Bog	CA	38.0782	−122.9555	6	2002	2005	−52	10,000	4.1	Anderson (2005)
42	Shutter Ridge Pond	CA	38.0517	−122.8014	35	2002	2005	−52	2200	4.1	Anderson (2005)
43	Mono Lake	CA	38.0071	−119.0123	1944	1987	1994	−38	>11,000	4.1	Newton (1991),Newton (1994)
44	Mono Lake	CA	38.0071	−119.0123	1944	2010	2020	575	10,900	5	Zimmerman et al. (accept.)
45	Glenmire	CA	37.9903	−122.7800	167	1998	2013	−48	7000	5	Anderson et al. (2013)
46	Mono Lake	CA	37.9893	−119.1383	1944	1986	1999	−35	13,340	5	Davis (1999a)
47	Coast Trail Pond	CA	37.9863	−122.7979	230	2002	2005	−32	15,000	4.1	Anderson (2005)
48	Greenstone Lake	CA	37.9800	−119.2930	3067	2001	2003	9700	14,700	5	Porinchu et al. (2003)
49	Wildcat Lake	CA	37.9683	−122.7853	62	1998	2005	−48	3200	4.1	Anderson (2005)
50	Swamp Lake	CA	37.9500	−119.8167	2756	2013	2012	−52	19,700	5	Street et al. (2012); Street et al. (2013); Smith and Anderson (1992); Smith (1989)
51	Tioga Pass Pond	CA	37.9083	−119.2583	3018	1985	1987	−35	10,500	4.2	Anderson (1987)
52	Ten Lakes	CA	37.9000	−119.5333	2743	1985	1988	−35	3630	4.2	Anderson and Davis (1988); Anderson (1987)
53	Lower Gaylor Lake	CA	37.8970	−119.3040	3062	1985	2010	−35	11,500	4.1	Hallett and Anderson (2010)
54	Siesta Lake	CA	37.8505	−119.6601	2430	1995	2003	−45	13,200	4.1	Brunell and Anderson (2003)
55	Mountain Lake	CA	37.7884	−122.4712	43	1999, 2000	2001	−50	1850	4.1	Reidy (2001)
56	Woski Pond	CA	37.7250	−119.6250	1212	1986	1991	−35	1390	4.2	Anderson (1987); Carpenter (1991)
57	Starkweather Pond	CA	37.6630	−119.0739	2424	1985	1990	−35	12,800	4.1	Anderson (1987); Anderson (1990)
58	Starkweather Pond	CA	37.6630	−119.0739	2424	2001	2008	10,500	14,500	5	MacDonald et al. (2008)
59	Barrett Lake	CA	37.5958	−119.0083	2816	1985	1990	−35	13,010	4.1	Hallett and Anderson (2010); Anderson (1987); Anderson (1990)
60	Barrett Lake	CA	37.5958	−119.0083	2816	2000	2008	10,500	14,000	5	MacDonald et al. (2008)
61	Nichols Meadow	CA	37.4245	−119.5792	1509	1989	1994	−39	17,490	4.2	Koehler and Anderson (1994)

Table 1 (*continued*)

Site #	Site Name	State	Latitude (°N)	Longitude (°W)	Elevation (m)	Year of core	Year of pub	Min age	Max age	Discussed in Section	References
62	Pearson's Pond	CA	37.3528	−122.2566	365	1970	1975	−20	3400	4.2	Adam (1975)
63	Lower Pahranagat Lake	NV	37.2167	−115.0814	1421	2012, 2016	2019	−62	5800	5	Theissen et al. (2019)
64	Balsam Meadow	CA	37.1613	−119.2525	2005	1983	1985	−33	13,000	4.2	Davis et al. (1985); Anderson (1987); Anderson et al. (1985)
65	Skylark Pond	CA	37.1739	−122.3140	268	2009	2013	0	3200	5	Cowart and Byrne (2013)
66	Dinkey Meadow	CA	37.0451	−119.1653	1683	1985	1988	−35	5600	4.2	Anderson (1987); Davis and Moratto (1988)
67	Exchequer Meadow	CA	37.0692	−119.1169	2219	1985	1988	pres	15,500	4.2	Davis and Moratto (1988)
68	Pinto Lake	CA	36.9567	−121.7709	34	1998, 2001	2006	−51	1240	4.1	Plater et al. (2006).
69	Owens Lake	CA	36.3954	−117.9590	1082	1997	1997	6700	15,800	5	Benson et al. (1997); Mensing (2001); Bradbury and Forester (2002)
70	Owens Lake	NV	36.3954	−117.9590	1085	1984	2000	70	1000	4.1	Li et al. (2000); Smoot et al. (2000).
71	Tulare Lake	CA	36.0000	−119.7500	64	1988	1999	−38	11,750	4.2	Davis (1999b); Atwater et al. (1986)
72	Tulare Lake	CA	36.0000	−119.7500	64	2005	2015	1800	19,000	5	Negrini et al. (2006); Blunt and Negrini (2015)
73	Silver Lake	CA	35.3400	−116.1100	693	2011	2015	1500	14,800	4.1	Enzel et al. (1989, 1992); Kirby et al. (2015)
74	Zaca Lake	CA	34.7778	−120.0392	730	2009	2014	−58	3000	5	Kirby et al. (2014); Feakins et al. (2014); Dingemans et al. (2014)
75	Lower Bear Lake	CA	34.2541	−116.9200	2059	2005	2012	476	9170	5	Kirby et al. (2012)
76	Dry Lake	CA	34.1206	−116.8282	2763	2003	2006	pres	9040	5	Bird and Kirby (2006); Bird et al. (2010)
77	Abalone Rocks Marsh	CA	33.9564	−119.9767	0	1994	1994	pres	5200	4.1	Cole and Liu (1994)
78	Lake Elsinore	CA	33.6733	−117.3542	377	2003	2010	150	9500	5	Kirby et al. (2019a, b); Kirby et al. (2013); Kirby et al. (2010); Kirby et al. (2007); Kirby et al. (2005); Kirby et al. (2004)
79	Soda Lake	CA	35.1418	−116.0567	284	2011	2019	9420	12,740	5	Honke et al. (2019)
80	Abbott Lake	CA	36.2310	−121.4824	260	2013	2016	0	1400	5	Hiner et al. (2016)
81	First Lake	CA	37.1264	−118.4839	3040	2005	2011	0	11,600	5	Bowerman and Clark (2011)
82	Second Lake	CA	37.1237	−118.4876	3061	2005	2011	0	6300	5	Bowerman and Clark (2011)
83	Las Trancas	CA	37.0878	−122.2591	178	1977	1981	5730	33,720	4.1	Adam et al. (1981)
84	Las Flores	CA	33.2833	−117.4583	6	1994	19,988	0	4800	4.2	Anderson and Byrd (1998)

latitude and also through time).

Unlike other cosmogenic nuclides, however, the amount of radiocarbon in the atmosphere at any time is also highly dependent on the incorporation of ^{14}C into molecules of CO_2 in the atmosphere, and incorporation of CO_2 into the Earth's carbon cycle (Hughen et al., 2004, 2006; Bronk Ramsey, 2008). These processes include uptake by the terrestrial biosphere; gas exchange with the surface ocean; and incorporation into soil carbon components; as well as release of ^{14}C-depleted CO_2 by burning of fossil fuels; by destruction or decay of terrestrial organic matter through deforestation and soil loss; and by exposure of deep-ocean water masses at the surface. As there is no a priori way to calculate the history of these processes in the Earth system, the ^{14}C content of a material can be translated into a true "calendar" year only by use of a calibration curve.

The existence of an offset between radiocarbon years and calendar years was recognized as early as the late 1950s (De Vries, 1958; Stuiver and Suess, 1966), and intensive effort was made by several radiocarbon labs in the 1960s to reconstruct the changes in atmospheric ^{14}C content and understand their origin (Damon et al., 1978). Radiocarbon measurements made on tree rings of known age from different geographical regions and by different laboratories began to enable calibration of radiocarbon dates, but it was not until the early 1980s that sufficient agreement existed to establish the first consensus calibration dataset, based on bristlecone pine and giant sequoia and reaching back 8000 years (Klein et al., 1982). Through the 1980s and 1990s additional tree species, laboratories, geographic regions, and sample types were added, culminating in the first IntCal curve in 1998 (Stuiver et al., 1998). Over the last two decades, IntCal has been continually refined and extended through the work of dozens of scientists, and incorporates radiocarbon dates on materials with independently estimated calendar ages, such as tree rings, macrofossils in varved lake sediments, corals, marine sediments, and speleothems (Reimer et al., 2013; Reimer et al., in press). An additional radiocarbon tool was introduced by atmospheric testing of nuclear weapons in the late 1950s and early 1960s, which nearly doubled the atmospheric inventory of ^{14}C between 1955 and 1964 (the "bomb curve," e.g., Hua et al., 2013). Excellent discussions of radiocarbon dating, the bomb curve, and the construction and application of the calibration curve can be found in Damon et al. (1978); Bronk Ramsey (2008), Hua (2009), and Reimer et al. (2013).

Originally measured by counting the beta particles produced by the decay of individual radioactive carbon-14 atoms (decay counting) (Taylor, 2016), radiocarbon dating began to shift to direct detection of carbon-14 atoms by accelerator mass spectrometry (AMS) (ion counting) in the years after a series of landmark papers in 1977 (Bennett et al., 1977; Muller, 1977; Nelson et al., 1977). In 1962, the radiocarbon community established A.D. 1950 as the year 0 for calculating radiocarbon ages, and committed to continuing to use the "Libby" half-life (5568 ± 30) rather than changing to the newly estimated value of 5730 ± 40 (the "Godwin" half-life) (Godwin, 1962). The difference between the two is accounted for in the calibration process and is one reason uncalibrated radiocarbon measurements should not be interpreted as ages. It should also be noted that the reference to 1950 CE as "present" is not necessarily the convention with other dating methods that report dates as "before present", and the potential impact is up to 70 years and growing: for example, Rasmussen et al. (2006).

In the early decades of radiocarbon dating, there was a considerable lack of standardization of nomenclature, in applying a correction for variations in the $^{13}C/^{12}C$ ($\delta^{13}C$) value of natural materials, and in calibrating measurements before interpreting them as calendar ages (Stuiver and Polach, 1977; Trumbore et al., 2016), and other aspects of radiocarbon dating. Although reporting generally became more consistent through the 1980s and 1990s, a

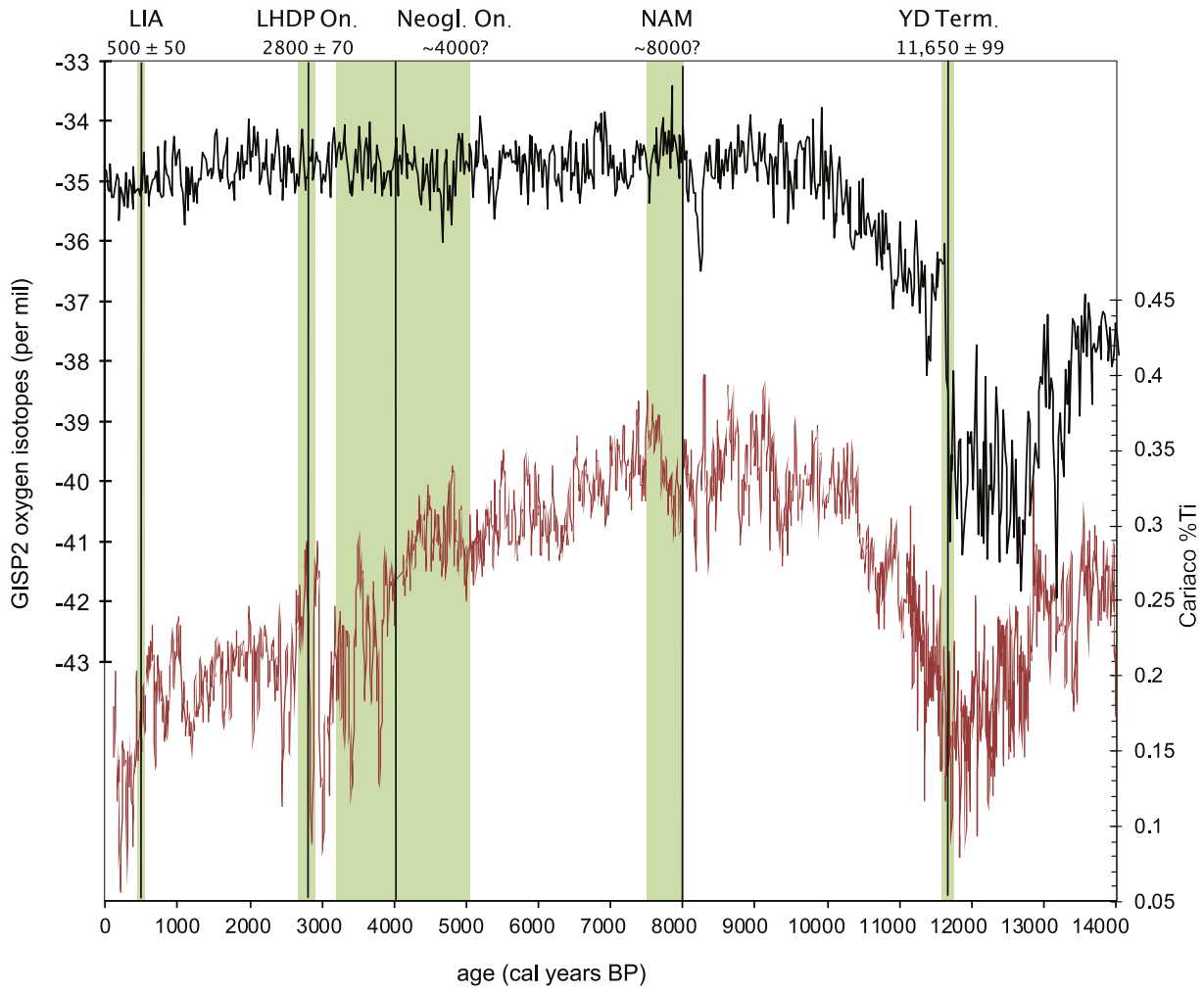

Fig. 2. Climate shifts of interest for the western U. S. during the Holocene Epoch, shown in the context of the GISP2 Greenland ice core record of North Atlantic conditions (upper panel; Stuiver et al., 1997) and the Cariaco Basin record of the tropical ocean-atmosphere (lower panel, Haug et al., 2001). The climate shifts are indicated by vertical black bars. The width of the green bars for the YD, LHDP, and LIA shows chronological uncertainties, while for the NAM and Neogl. it represents the range in age of climate proxy shifts in various records. The termination of the Younger Dryas (YD) cold period is quite abrupt and well dated in Greenland ice cores (11,650±99 cal yr BP; Walker et al., 2009); the modern North American monsoon (NAM) is proposed to have developed between ~8000 and ~7500 cal yr BP (Barron et al., 2012); the Neoglaciation (Neogl.) is suggested to have begun in the Sierra Nevada as early as >5 ka (Owen et al., 2003) and as late as ~3200 cal yr BP (Bowerman and Clark, 2011), while lakes indicate a significant shift toward wetter conditions at various times between 3800 and 3000 cal yr BP (Zimmerman et al. accepted); the Late Holocene Dry Period (LHDP) is best defined at Stonehouse Spring, NV, with onset at 2800 cal yr BP (±70 yr; Mensing et al., 2013); the beginning of the Little Ice Age (LIA) is defined at about 500 cal yr BP (1450 C E; Masson-Delmotte et al., 2013), but with significant record-to-record variability (which we have estimated here as ± 50 yr).

recent review of papers published in 2018 and 2019 by Lacourse and Gajewski (2020) found that a third did not report some essential information (AMS vs decay-counting, the material dated, the name of the ^{14}C lab, or the lab ID numbers for each sample). Nearly a quarter of the 62 studies (reporting 80 new age models) did not report what calibration dataset was used. In fact, many studies into the late 1990s and early 2000s still discussed paleo-environmental records in uncalibrated ^{14}C years (e.g., Anderson and Byrd, 1998; Davis, 1999a; Fritz et al., 2001). In all cases users of published records must pay careful attention to whether, and how, the ages were calibrated.

It is important to note that the difference between radiocarbon years and calendar years is not a simple offset. Over the last 2200 years, radiocarbon years have been both younger and older than calendar years at various times (Fig. 3). The difference between radiocarbon years and calendar years steadily increases from zero offset at about 2200 years ago to a 2000-year offset at about 12,500 years ago, with radiocarbon years growing generally younger than calendar years over that interval. The impacts are several-fold: first, rates of change, the real timing and duration of events, and impressions of synchrony or diachrony calculated using radiocarbon years will be incorrect (Bartlein et al., 1995); second, even correlations between two records dated by radiocarbon are likely to be incorrect, because the offset is non-monotonic (e.g., between 4000 and 6000 ^{14}C years ago, Fig. 3); third, correlation between radiocarbon-dated records and records dated by other methods (e.g., ice cores, speleothems, glacial features) will essentially always be incorrect.

Additionally, the non-linearity of the calibration curve means that most frequently there is no single time period of calendar years that corresponds to a particular radiocarbon age. On decadal timescales, the relationship between radiocarbon years and calibrated years “wiggles,” with many reversals, periodic plateaus, and occasional steep slopes (Fig. 3). This results in a typical radiocarbon date (in the Holocene, with 30-year 1-sigma Gaussian analytical uncertainty) having a complex probability distribution of calibrated years. Although this can cause large and discontinuous age spreads that are unwieldy to handle, the calibrated age range describes all

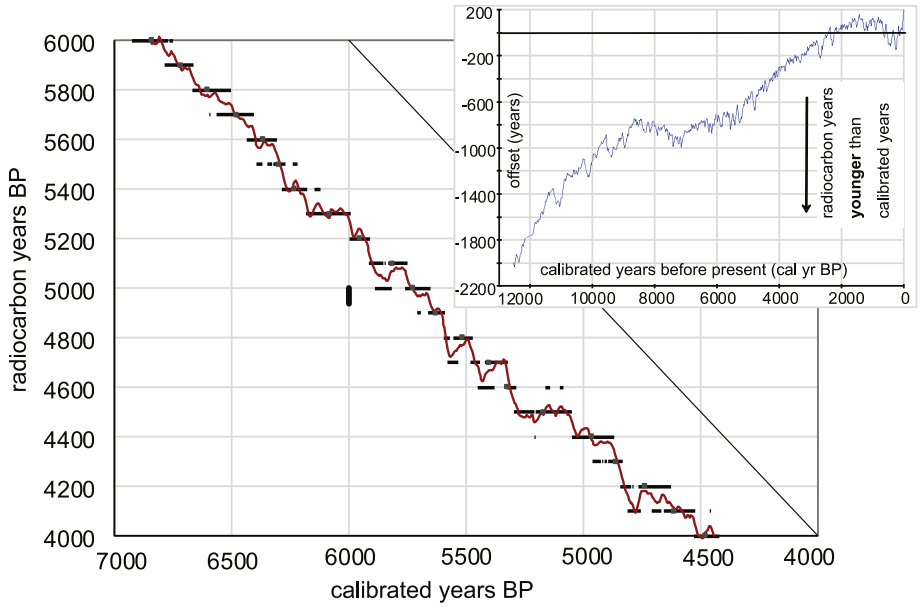

Fig. 3. Relationship between radiocarbon and calibrated years for the period between 6000 and 4000 radiocarbon years BP. The red line indicates the IntCal13 radiocarbon calibration curve (Reimer et al., 2013); horizontal black bars show the 2-sigma range in calibrated years BP of ^{14}C measurements at 100-year intervals with typical ±30-yr 1-sigma uncertainties (example shown in vertical black bar). Solid black line shows the 1:1 relationship between ^{14}C and calibrated years. Inset shows the offset between radiocarbon and calibrated years BP over the last 13,000 years: horizontal black line indicates zero offset.

of the time windows in which the atmosphere contained the radiocarbon content appropriate to produce the measured value. Thus, the 2-sigma (95%) time windows should be used for a calibrated age, even those with low probability. Typical uncertainties for calibrated radiocarbon ages in the Holocene are on the scale of 100–200 years when the full 2-sigma range is considered.

Several factors need to be considered when assessing the suitability of material for radiocarbon analysis. As mentioned above, organic material can be pre-aged on the landscape for an unknown amount of time prior to being deposited in the sediment. This may include materials such as pollen, charcoal, and organic compounds such as leaf waxes that were deposited in soils or lake sediments from higher-elevation deposits (e.g., from an earlier highstand) and subsequently eroded. Sediments can also be reworked within a lake before being redeposited in sediment of a younger age, or, alternatively, mixed into older strata from above as a result of bioturbation. Material can also be displaced during coring, and macrofossils near the core edge or at the top or bottom of separate drives should be viewed initially with skepticism. Pieces of wood may come from parts of a tree that was decades or centuries old when it died, possibly spending a similar amount of time decomposing on the landscape before it was deposited. Contribution of old groundwater from large regional aquifers, flow along faults, or release of groundwater stored under large lakes after lake-level drop can add ^{14}C-depleted water to a lake or meadow, creating a reservoir effect of unknown and temporally variable quantity when that carbon is subsequently fixed by aquatic plants or used to construct carbonate shells (Deevey et al., 1954). Although these are not necessarily a priori reasons not to date a particular material, they are factors that must be weighed in assessing the resulting radiocarbon measurements.

2.2. Tephrochronology

Due to its location along a plate boundary, the western US has been volcanically active over the last ~15 million years, with the region from California to Washington state characterized by explosive silicic volcanism (John et al., 2012). Individual volcanic eruptions are geologically short-lived events (days to several years) and tephra are often spatially widespread. As a result, individual airfall tephra layers can be highly useful in creating regional isochronous timelines. The first step in using tephras as chronomarkers is to uniquely identify a tephra, typically using geochemical techniques, though mineralogic and morphologic characterizations are often carried out as well (Davis, 1977). Many volcanic systems evolve chemically over time, producing tephras with a chemical "fingerprint" that can be identified by analyzing the major- and minor-element chemistry of constituent components, typically glass shards (Lowe, 2011; Knott et al., 2018). Identifying a tephra based on chemical and other analyses doesn't provide an age, however. Age information associated with an eruptive event must be collected from deposits where the tephra occurs (e.g., radiocarbon, biostratigraphy), or directly measured from co-magmatic crystals found in the tephra (e.g., by $^{40}Ar/^{39}Ar$ dating (Chen et al., 1996) or (U–Th)/He (Cox et al., 2012)). The process of dating a tephra is often iterative, with several instances of a tephra deposit providing independent age information. This can result in a robust understanding of an eruption's age, which can then be applied to any sediment sequence that contains the same tephra, once it has been chemically identified. A good example of this is the Mazama tephra, produced during the climactic eruption of Mount Mazama, Oregon, which is found across a wide swath of the western US. The Mazama tephra has distinctive glass chemistry and is associated with dozens of radiocarbon dates in a variety of terrestrial deposits (Egan et al., 2015). As a result, positive identification of the Mazama tephra in a sediment sequence can allow it to serve as a distinct, well-constrained chronomarker. While Egan et al. (2015) are able to constrain the 95% uncertainty window of the Mazama tephra to 98 years, uncertainties of tephra ages in the Holocene are commonly on the order of multi-centennial.

In contrast, some tephras are less distinguishable based on their chemistry, leading to confusion in compiling ages (e.g., the Turupah Flat bed (Adams, 2003)). Eruptions from the Mono-Inyo Craters have deposited tephras in locations across the Great Basin, but

unfortunately the tephras are indistinguishable using glass chemistry. As a result, many studies in the region cite the occurrence of a "Mono Craters-type" tephra, but cannot be more specific about which. In some cases, the authors may speculate as to its age (e.g., Hallett and Anderson, 2010), but outside of the Mono Basin (and often within: Davis, 1999a) the occurrence of such a tephra cannot add independent age information. Within the Mono Basin, the two youngest tephras are frequently exposed in outcrops and research pits, have distinctive stratigraphy and other characteristics, and are well dated by associated organic material (Sieh and Bursik, 1986; Bursik and Reid, 2004; Millar et al., 2006; Bursik and Sieh, 2013; Bursik et al., 2014) to 600 cal yr BP and about 1350 cal year BP. Recent groundbreaking work by Marcaida et al. (2014, 2019) has demonstrated that the Pleistocene eruptive products of the Mono Craters can be distinguished by the major-element composition of their titanomagnetites, and it may be that the titanomagnetite chemistry can also uniquely identify the Holocene tephras as well.

2.3. Historical-period indicators

It is particularly important to have the age of recently deposited material determined as accurately and precisely as possible, because proxy data from these sections are often calibrated to the instrumental record in order to better understand the relationship between proxies and environmental variables. The arrival of European settlers in the western US is relatively recent, between the 18th and 19th centuries, and can often be traced in a particular location through property deeds, newspapers, family papers, and other written sources. This can be useful in assessing the age of the youngest sediments in a core, because non-native plants often arrived with European settlers. Many of these non-native plants are weedy taxa that thrive in ecologically disturbed landscapes and produce abundant pollen. Historical botanical collections can be used to help constrain when various non-native plants arrived in different areas and, when pollen from these plants is found in a sediment sequence, its deepest occurrence can be used as a chronomarker (e.g., Kirby et al., 2004; Reidy, 2013).

Sediment from the historical period can also be dated by measuring the abundance of radioisotopes ^{210}Pb and ^{137}Cs. Many short-lived isotopes were generated in the atmosphere by nuclear-weapons testing in the late 1950s and early 1960s, and the ^{137}Cs isotope (half-life 30.17 yr) has been widely used to identify the level in a sediment core corresponding to the first appearance of ^{137}Cs, around 1952, as well as the peak of the global atmospheric testing and ^{137}Cs levels around 1963 (Drexler et al., 2018). ^{210}Pb has a half-life of 22.23 years and is formed in the environment as part of the ^{238}U decay chain (Appleby et al., 1979; Appleby, 1998). As such, it is useful in providing age information for sediment that is around 100–150 years old. In sedimentary deposits, ^{210}Pb comes from two sources: as an in situ natural decay product of its parent isotope (^{226}Ra) found in local rocks, and from the decay of atmospheric ^{222}Rn with subsequent deposition and incorporation into the sediment matrix. The first source comprises "supported" ^{210}Pb, and the latter "unsupported" or "excess" ^{210}Pb. Once ^{210}Pb has been measured in recent sediment, the investigator must choose between several models that use different assumptions about the supply of excess ^{210}Pb and the activity (concentration) of the supported ^{210}Pb to derive an age-depth model. Because of this model dependence, it is highly beneficial to have a secondary chronomarker (ie, exotic pollen or ^{137}Cs) to verify assumptions in ^{210}Pb models. Modeling recent ages using these radiometric approaches, one must consider analytical and geological uncertainties as discussed above (Barsanti et al., 2020; Sanchez-Cabeza and Ruiz-Fernández, 2012). Dating uncertainties associated with historical-period techniques are typically on the order of decades.

3. Building a robust chronology

3.1. Core stratigraphy

The first requirement for building an age model or assessing a published age model is documentation of the underlying coring methods and a basic description of the cores used for the study. A frequent problem with many older studies is the lack of information about the methods used to retrieve and preserve the core(s). Significant information includes whether the core was recovered in a single drive or multiple drives, whether compaction was observed, and if any gaps in sediment recovery exist between drives (e.g., Cole and Liu, 1994; Kirby et al., 2010). The most robust studies rely on two overlapping cores taken in the same campaign a short distance apart. Indeed, this is the only way to assess the percent recovery of the sediment column without relying on assumptions about the accuracy of field depths and the degree of compaction or expansion of various lithologies that may have occurred during the coring process. When overlapping cores are taken, the method(s) of correlation and depths of key tie points between the cores should be reported, as well as the section and section depth of the age control points. Even a brief description of the sediment cores should include any observed disturbance that can be attributed to the coring, especially missing or disturbed sediment at the top or bottom of a drive (e.g., Thompson et al., 2016).

In many studies the top of the core is assigned the year of coring, but this inference needs to be supported by discussion of how the sediment-water interface was captured, including whether a gravity core or surface block (for a meadow) was associated with the coring and how disturbance of the interface was minimized during core collection, transport and storage. The use of historical-period chronomarkers, or proxy evidence of a known environmental event (e.g., flood or fire) to constrain the age of recent sediment is useful to verify that the core top has been captured and preserved.

These hurdles to constructing a robust - and revisable - age model are less of a challenge in recent studies, which often include good quality images or additional core description (although sometimes buried in a supporting information file). Unfortunately, Lacourse and Gajewski (2020) found that two-thirds of the recent studies they surveyed assigned the core top to the year of collection, but 86% of those studies provided no details to support that inference, and 40% of all the studies failed to even report the year of core collection. In studies where this information is not reported, the lack of detail represents a significant barrier to assessing the age of the upper sediment and associated proxy data, and may prevent the data from being included in other studies.

3.2. Methods for interpolation and extrapolation

Age models have traditionally been constructed by fitting a linear, spline, or other function through a series of dates represented as single points with (usually symmetrical) uncertainties. The review of Lacourse and Gajewski (2020) found that 42% of recent age models they surveyed were linear interpolation or spline fit. However, the complex probability distribution of calibrated radiocarbon dates makes it impossible to accurately represent the full range of possible calibrated ages with this method. Furthermore, it is also impossible to estimate the uncertainty in the age of any sediment interval *between* measured ages by any simple technique. One effect of this approach is that sedimentation-rate changes often occur artificially at the location of measured dates, whether or not there is any indication of a change in sedimentation

at that point. Moreover, models built using these methods often don't account for stratigraphic contacts where changes in sedimentation rates are expected. Several comparisons of techniques for modeling the accumulation of sediments show that classical methods produce false confidence in the age model, because they appear to be highly certain, especially at typical dating densities of less than one date per 1000 years (Telford et al., 2004; Trachsel and Telford, 2017; Blaauw et al., 2018).

The most practical and rigorous way to address these issues is to use a Bayesian-based program to build an age model. The Bayesian approach combines prior information such as stratigraphic or spatial relationships from the investigator and the full probability distribution of each age control point from the calibration curve to iteratively define all possible age models, using Markov Chain Monte Carlo (MCMC) sampling (often with millions of iterations). Age models that violate the stratigraphic or other bounds set as priors are rejected, and the remainder statistically describe the probable age range for a sediment sequence. For thorough and quite readable discussions of Bayesian statistics and their application to chronologies, we highly recommend Bronk Ramsey (2009) and Parnell et al. (2011).

The most widely used programs for implementing this approach are OxCal (Bronk Ramsey, 1995; Bronk Ramsey and Lee, 2013), BChron (Haslett and Parnell, 2008) and Bacon (Blaauw and Christen, 2011). Although the underlying approach of all three programs is Bayesian, the specific mathematical methods and user interfaces vary. For example, OxCal was developed to meet the needs of archaeologists, who often date multiple materials that may be associated with the same event or sequences that may have large gaps in time. Bacon was developed to model the accumulation of sediment more or less continuously in a wetland, lake, or other terrestrial (or marine) basin, as well as being quite user-friendly, and so we prefer it for our purposes.

Bacon (Blaauw and Christen, 2011) models the accumulation of sediment using prior information provided by the investigator about a sediment sequence, including the consistency of sediment accumulation (memory), hiatuses, turbidites, missing core section, and tephras or other interruptions to steady accumulation. These priors are used in combination with the complete probability density function of calibrated radiocarbon ages and other chronologic inputs. Nearly any type of age control point can be used as input, including core-top age, exotic pollen, ^{210}Pb, tephras, radiocarbon ages, and U-series ages. Caution must be applied when combining ^{210}Pb ages with other methods: because ages produced with the ^{210}Pb method are modeled, usually outside of and prior to use of a Bayesian program, significant artificial breaks in accumulation rate can occur at the intersection of the ^{210}Pb ages and the other age control. This problem is treated more fully in Aquino-Lopez et al. (2018), where Plum, a Bayesian age-modeling program constructed to incorporate raw ^{210}Pb data with raw data from other age control methods, is presented. Millions of age-depth models are then constructed from estimation of the accumulation rate of many small sections of core (typically 5–10 cm thick, chosen by the investigator) and models that contain reversals are rejected.

The use of Bayesian programs has several significant advantages over classical age modeling: first, Bayesian age modeling considers the full complexity of the calibration curve encompassed by the radiocarbon dates. Whereas the analytical uncertainty for a radiocarbon measurement (like other isotope measurements) is Gaussian, the non-linear shape of the calibration curve produces an irregularly shaped, often highly asymmetrical, probability distribution. In some cases, there are two or more probable age ranges, separated by periods of no probability (Fig. 3). To express such age information as a simple point estimate age (i.e., mean or median) with symmetrical uncertainties is not merely inaccurate, but results in misleading age information about the associated data.

A second advantage of Bayesian age modeling is that the iterative procedure defines the uncertainty in the age model between dates, so that not only the *age* of any event in the record can be identified, but the *precision* with which that age is known can be identified as well. In this way, the confidence with which we can infer that changes observed in separate archives occurred at the same time can be quantitatively assessed. In some cases this may help to identify – or eliminate – a hypothesized driving mechanism or spatial pattern.

An additional strength of Bacon is the ability to define where additional dating may be most effective. Producing a final age model is often an iterative process, with each new date providing information that further constrains uncertainties and identifies sections of the core that would benefit from more age control. Blaauw et al. (2018) present a quantitative approach for determining depths at which additional age control will most benefit the model by calculating the depths with the largest uncertainties. This approach also considers which depths will benefit with regard to providing the most information about other depths in the core. Using sequences with known ages from varve counts to test the impact of additional ages, they show that Bayesian-based age-modeling approaches increase in both precision and accuracy with additional dates (as opposed to classical age modeling techniques) and provide more confident reconstructions. Ultimately, they suggest that at least 2 dates per millennium are needed for precision at the centennial timescale, with more than 50 dates per millennium needed for decadal confidence in age model precision! Sections with proxy changes of particular interest or distinct stratigraphic contacts will benefit from more dates to better constrain the timing or rate of significant changes (Thompson et al., 2016; Zimmerman et al., accepted).

4. Sedimentary records of western U.S. paleoclimate from lakes and meadows

We identified 84 records for the region that reconstructed some portion of the last 12,000 years, in the published literature, available theses and dissertations, and various non-peer-reviewed reports (Fig. 1, Table 1). In order to assess the quality of the age models, age control data were drawn from tables and comments in the original studies, and the locations of hiatuses or other disturbances and assessment of the quality and relevance of the dates follows that of the original authors. An exception was made for studies with a tephra layer attributed to the Mazama eruption; in this case, we used an age of 7635 ± 50 cal yr BP, based on the recent assessment of all ages associated with the Mazama tephra by Egan et al. (2015). For locations with multiple studies over time, publications associated with the same cores were grouped together (e.g., Dingemans et al., 2014; Feakins et al., 2014; Kirby et al., 2014), while studies using different locations or sets of cores at the same site were assessed separately (e.g., Anderson, 1990 versus MacDonald et al., 2008; Davis, 1999a versus Zimmerman et al. accepted).

4.1. Records with insufficient dating

Our results show that the ability to reconstruct past climate changes in the western U.S. at sub-millennial time-scales is currently severely limited, due to the fact that many published records have sparse age control. This results in age uncertainties that are suitable only for millennial- or orbital-scale interpretations; in fact, at the time many of the studies were performed, those were the time-scales of interest, and decay-counting was the main tool for chronological control.

Of the 84 records, 3 were too short for our analyses (<2000

years). An additional 20 could be categorized as having too few dates to adequately constrain the sedimentation history of the core. Ten records had between 0 and 5 age control points, often a mixture of decay-counted bulk dates and an AMS macrofossil date, and one or more unidentified tephras (Table 1). Another 10 records had 5 or more dates, but those dates were distributed between many cores or drives with stratigraphic uncertainties (Kirby et al., 2015; Thompson et al., 2016); were clustered, leaving large gaps (Starratt et al., 2003; Osleger et al., 2008); or contained reversals making interpretation difficult (Minckley et al., 2007). These 23 records were not considered further in this study.

4.2. Records with only decay-counting radiocarbon dates

A second set of sites with insufficient age control is composed of sequences whose only age control is decay-counting radiocarbon dating of bulk sediment (n = 19), mostly studies performed in the 1970s, 1980s, and early 1990s (including some published into the late 1990s and early 2000s). While decay-counting techniques are no less precise or accurate analytically than AMS dating (Stuiver, 1978; Hogg et al., 2006), the requirement of three orders of magnitude more carbon than AMS analysis reduces the geological precision of the measurement in two ways.

First, of the 19 sites reviewed here that were dated only with decay counting, all used bulk sediment samples that were generally 5–15 cm thick, with some as thick as 25–30 cm. In some cases no sample thickness was reported, a problem which persists even in recent studies (Lacourse and Gajewski, 2020). With average sedimentation rates on the order of 25–30 cm per kyr, these samples integrate sediment deposited over hundreds of years into a single date.

Second, and more significantly, bulk-sediment dates introduce uncertainty in the source and age of the carbon being dated. Although it is often argued that bulk-sediment dates are not affected by old carbon (reservoir effect) at a study site because the surrounding bedrock is not carbonate, this is not the only process that can decrease the ^{14}C content of the carbon in lake sediments. As mentioned in section 2.1, old groundwater can provide ^{14}C-depleted carbon that is taken up by aquatic plants, and reworking of fine organic material can result in inaccurate ^{14}C ages. Furthermore, carbon incorporated into aquatic biomass and deposited on the lake bottom can be recycled into the dissolved carbon pool in the lake and reused by aquatic organisms for both carbonate shells and organic material. Bulk-sediment dates may also reflect the inclusion of particulate and microfossil carbon eroded from the surrounding landscape (Howarth et al., 2013; Gierga et al., 2016; see section 5.3 for fuller discussion).

Each of these sources of carbon may have a different ^{14}C content, not necessarily equilibrated with the coeval atmosphere. Both the offset between the atmosphere and any carbon source, and the fraction of the total carbon contributed by the different sources, may change through time. Pretreatment in the laboratory can remove some forms of unwanted carbon (e.g., hydrochloric acid treatment to remove carbonates), but few of the early studies reported any details of sample preparation before radiocarbon dating. For example, Foit and Mehringer (2016) reported that samples from Diamond Pond were treated with NaOH and HCl to remove carbonates and humates before dating, but this information is not noted in the original publication (Wigand, 1987). Finally, there is no check against any independent age control in any of the sites reviewed that were dated with decay counting, with the exception of two sites where the Mazama and Tsoyowata tephras were identified by elemental chemistry (Edlund and Byrne, 1991; Smith and Anderson, 1992).

4.3. Two classic records: Walker Lake and Pyramid Lake

A typical example of a record dated only with decay counting is the Walker Lake core WLC84-8, studied by Benson et al. (1991), Bradbury et al. (1989), and Meyers and Benson (1988), where the authors inferred the lake-basin history from carbonate geochemistry, stable isotopes, diatoms, and pollen. The core was dated by 6 decay-counted radiocarbon dates on bulk sediment, and the core top was assumed to be modern. As with many early studies, no information to support that assumption is given. In this case, details of the sediment pretreatment and the $\delta^{13}C$ correction can be found separately in the radiocarbon date list reported by Yang (1988). The reported ages have 1-sigma uncertainties of ±110–220 years (2-sigma uncertainties of ±220–440 years and thus 95% uncertainty ranges of 440–880 years, before calibration), but the sediment samples also integrate between 15 and 25 cm of core. The very high sedimentation rate for this core (1100 cm in ~4000 yr) means that the dated samples may integrate only ~70 yr each, but in records with lower sedimentation rates the time integrated with this approach is much larger. For example, in a more typical 250 cm-long core covering 8000 years, a 15 cm-thick sample will integrate 480 years. Furthermore, as is common in decay counting-dated records, the ages discussed in Benson et al. (1991) are reported in "yr BP" - *uncalibrated* radiocarbon years. Thus, the two desiccation events noted at 5300 to 4800 yr BP and 2700 to 2100 yr BP have calibrated ages of 6105 to 5585 cal yr BP and 2780 to 2105 cal yr BP, likely with an uncertainty of ±300–500 years. Finally, the sources of the carbon in the bulk sediment samples that were dated remain unknown, leaving the accuracy of the age model impossible to assess.

The Pyramid Lake, Nevada, record is widely cited and has had a significant role in shaping the general view of Holocene environmental changes in the eastern Sierra and Great Basin, yet the age control is too complex to be modeled. The isotope and pollen records of Benson et al. (2002) and Mensing et al. (2004) from Pyramid Lake have been widely cited since their publication (combined citations >300) because they provide a rare view of Holocene vegetation and aquatic conditions in the arid plain that was part of Lake Lahontan during the last glacial period. The records were developed from a set of three cores, two piston cores and a box core, taken in 1997 and 1998 from near the center of the lake (water depth ≥100 m). An age model was constructed for the box core (PLB98-2, 0.59 m long) using four horizons: i) the core top, assumed to be close to the date of recovery; ii) the peak in ^{137}Cs (1964 CE); iii) the first appearance of ^{137}Cs (1952 CE), and iv) the appearance of mercury, related to the expansion of ore processing in the region in 1860 CE.

The piston cores (PLC97-1, 5.35 m and PLC98-4, 6.34 m) were analyzed with radiocarbon on pollen separates (PLC97-1, n = 8) and on the total organic carbon (TOC) fraction of the sediment (PLC97-1, n = 6; PLC98-4, n = 30). The table presenting the pollen-based dates (in Benson et al., 2002) refers to Mensing and Southon (1999), suggesting that the separates were prepared by the chemical and physical purification methods used in that paper. Likewise, the chemical pretreatment of the bulk sediments is also not described; however, presumably it was similar to the standard rinsing and HCl acidification treatment described by Benson et al. (1996).

Several lines of evidence were used by Benson et al. (2002) to argue that all the radiocarbon dates on both cores were likely too old. First, radiocarbon dates on modern aquatic samples from Pyramid Lake showed a 600-year reservoir effect in the late 1950s (Broecker and Walton, 1959). Second, radiocarbon measurements on the TOC fraction of the 30 down-core samples from core PLC98-4 showed significant scatter relative to a linear depth-^{14}C line. This

scatter was interpreted to represent reworking of older sediment around the lake into the lake basin. The reworking of older sediments from shallow to deep water was also indicated by the increasing age of lake-bottom sediments down to about 85 m water depth, below which two core tops showed modern ages. X-radiographic evidence for burrowing organisms in the sediment column sampled by the cores lent additional evidence against relying on bulk radiocarbon ages. Thus, the age model for PLC98-4 was constructed using a polynomial fit to the four TOC measurements forming the youngest edge of the age-depth line, which were adjusted by 600 years.

The age model for the PLC97-1 core relied instead on correlation of features in the paleomagnetic secular variation (PSV) record to PSV features recorded by archaeomagnetic samples (ARCMAG) compiled by Lund (1996). The ARCMAG samples record a thermal remanence from hearths and lava flows, making them highly reliable recorders of the magnetic field, and were dated by decay-counting radiocarbon measurements on wood and other macroscopic organic material. The period used for the PLC97-1 age model, since about 2500 ^{14}C yr BP (2700 cal yr BP), has the highest density of samples and thus the best definition of peaks and valleys in the ARCMAG PSV curve, yielding 6 inclination and 6 declination features. However, Benson et al. (2002) list 16 tie points between the PLC97-1 core record and ARCMAG, and the Pyramid Lake PSV curves and the correlation used to identify and correlate the features have not been published. Benson et al. (2002) consider the PLC97-1 age model accurate to within 50–100 yr, but without the primary PSV curves, the precision of the correlation – and the possibility of alternative correlations – cannot be tested (e.g., Zimmerman et al., 2006; Lund and Platzman, 2015). Like every wiggle-matching exercise, independent constraints may reduce the number of possible correlations, but multiple possibilities may remain.

Further, the precision of the PLC97-1 age model can be no better than the precision of the ages for the PSV records to which the core was correlated. The age uncertainty reported for the ARCMAG features identified by Lund (1996) is between ±75 and ± 175 years; since the ages are reported in radiocarbon years, these are most likely 1-sigma uncertainties. Thus, the 2-sigma uncertainty of the ARCMAG features is ±150 to ±350 years, before calibration to calendar years. Full consideration of the uncertainties identified here suggests that the precision of the PLC97-1 age model is likely no better than ±500 years (95% range = 1000 years). Finally, in addition to being dated by separate methods, the PLC98-4 and PLC97-1 cores do not overlap in time (as noted by Benson et al., 2002), leaving the temporal relationship between their records uncertain.

5. Age model assessment for the better-dated studies

5.1. Construction of Bacon models

In order to assess the temporal uncertainty of changes observed in the proxy data from the remaining 42 sites, we constructed a new age model for each record with Bacon (Blaauw and Christen, 2011), using the rbacon package, v.2.3.9.1. We used as input the age control points, hiatuses, and other stratigraphic or chronologic information that was provided by the original authors. Because ^{210}Pb age control is based on the age-depth relationship for samples modeled as a set, we used the modeled age and depth for the deepest sample as a single age-control point, with an assigned uncertainty of 10 years based on the range of uncertainties reported in the original papers. Bacon has several parameters that can be varied in pursuit of the most robust age model; the parameters used for each age model analyzed here can be found in Supplemental Table 1. In general, we used the following guidelines:

1. *Section modeled*: Bacon models were constructed for the section described and sampled by the authors, which sometimes was less than the total sediment collected. In other cases, the authors interpreted data from core sections below the deepest age control point, requiring extrapolation of the age model. For cores that extended back into the last glacial period, the Bacon model included dates just before the beginning of the Holocene Epoch, to help to guide the age model into the Early Holocene.
2. *Bacon values*: To begin, all sequences were modeled using the default Bacon values (Table 3). The most common modification was for the mean accumulation (acc.mean), usually to a round number close to the yr/cm (5, 10, 50, 80, or 100), estimated roughly from the depth and (^{14}C) age of the deepest date. Another common variation was changing the thickness of the modeled sections. In some cases, thick was reduced to 3 cm or increased to 10 or 20 cm to guide the age model toward dates spaced closer together or farther apart. In no case did changing the acc.shape or mem.mean improve any age models; in a handful of cases, changing the mem.strength or number of MCMC models stored ("ssize", default 2000) improved the fit or stability of the model.
3. *Stratigraphic interruptions*. In two cases, the original core stratigraphies were modified by the original authors to account for thick tephras (Zimmerman et al., accepted) or instantaneous events (Bird et al., 2010). In all other cases the tephras noted by the original authors were <5 cm thick and were not removed from the stratigraphy in the original publication. The sediments in Owens Lake core OL84B were modeled with a hiatus at 225 cm, as noted by Benson et al. (1997). The age of the gap in our model is 6735 (±330/450) to 4720 (±450/315) cal yr BP, close to the age listed in the original publication (~6.7–4.5 ka in the text, 6.1–4.3 ka in the figure; Benson et al., 1997). Hiatuses were also suggested by the dates at Glenmire (Anderson et al., 2013) and Mono Lake (Zimmerman et al. accepted); in both cases, the authors did consider the possibility of a hiatus, but did not include one in the original age model. The Bacon model we produced for Glenmire requires a hiatus in order to capture the oldest date; however, increasingly complex interpretation of age data such as this requires close examination of the core, which is outside the scope of our study, and so we include only the upper section in our analysis, similar to the original study.

When an age model was reached that represented the age control and stratigraphic description provided by the authors (Supplemental Table 1), we calculated the width of the 95% uncertainty window down- core by subtracting the minimum age from the maximum age for each depth, at 1 cm intervals. This represents the full width of the 95% uncertainty envelope (e.g., ±100 yr has a 95% uncertainty envelope of 200 years). All ages quoted here are the mean age reported by Bacon; age-depth plots developed by Bacon and plots of downcore uncertainty for all models can be found in Supplemental Figure 1.

To better understand how well constrained proxy-data changes are in these records, we also calculated the 95% uncertainty ranges for all zone boundaries or environmental shifts (hereafter: zone/event boundaries) reported in the original studies. Many pollen and other biological studies use cluster-analysis techniques to identify zone boundaries, where assemblage data show a distinct change to different overall conditions (e.g., Dingemans et al., 2014; White et al., 2015). Event boundaries were typically identified in geochemical or sedimentological proxies as discrete shifts in the proxy data to different environmental conditions such as pluvials (e.g., Kirby et al., 2010) and droughts (Mensing et al., 2008). Core tops were included as zone boundaries. In the case of Starkweather Pond and Barrett Lake (MacDonald et al., 2008), the known age of

the Younger Dryas period was used as an event within which proxy data were interpreted. The core depths of zone/event boundaries were used to apply ages and 95% uncertainty ranges from the new Bacon models. If no depths associated with boundaries were reported in the original publication, they were determined, when possible, through the use of publicly available data (from the Neotoma and National Center for Environmental Information databases). We analyzed zone/event boundaries for 30 sites; the remainder either lacked a discussion of distinct events or zones, or we were unable to find the needed core depth. A total of 190 boundaries was used in the analyses.

5.2. Patterns of precision

Overall, the 42 newly created Bacon age models have an average 95% uncertainty of 594 years, with an average standard deviation of 291 years (48%) (Table 2). Fig. 4 shows the percentage frequency of uncertainties in 200-year bins for entire records (mean) and at different time slices through the Holocene. Overall, 57% of the 42 records have mean uncertainties of 600 years or less. The time-slice frequencies clearly show lower uncertainties in the late Holocene, with a larger percentage of ages from before 6000 years ago having >600-year uncertainties than after (49% vs 23%). For example, the 10,000-year time slice shows that more than 70% of the available records have uncertainties of greater than 600 years, while at 2000 years ago, only 30% of available records have uncertainties >600 years (Fig. 4).

The effect of these uncertainties on climate correlations can be seen when the uncertainty ranges are plotted alongside the Cariaco Basin record of the ITCZ position (Haug et al., 2001). Fig. 5 shows the uncertainty range for each available record at the five time slices described in section 1. The 21 records that cover the end of the Younger Dryas, for example, have a mean uncertainty of 946 years. Of those 21, 9 have uncertainty ranges of >800 years at 11,650 cal yr BP, while the whole YD period is only 1200 years from beginning to end. The precision is much better for the shift from the MCA to the LIA, with a mean uncertainty of 338 years (n = 32). However, even this level of uncertainty prevents the making of important comparisons, such as distinguishing between the onset of the second major Medieval drought defined by Stine (1994) at ~740 cal yr BP (1210 CE) and the intensification of Little Ice Age glaciation observed by Miller et al. (2012) at ~500 cal yr BP (1450 CE).

There is no apparent relationship between the mean uncertainty and either the number of dates in a study or the number of dates per meter (Fig. 6a and b). However, the relationship between the mean uncertainty and the number of dates per thousand years is striking. Fig. 6c shows an exponential relationship, with fewer

Table 2

Site No.	Site	n dates	length (cm)	length (# of yr)	dates/m	dates/kyr	mean 95%	std. dev.	% std dev	max 95%	min 95%
4	Hobart Lake	12	1147	7282	1.0	1.6	284	104	36.6	497	50
5	Bolan Lake	12	789	13,904	1.5	0.9	544	215	39.5	98	58
7	Bear Lake (96–2)	10	300	13,793	3.3	0.7	818	322	39.4	1479	268
8	Sanger Lake	24	605	13,717	4.0	1.7	430	233	54.2	1485	47
9	Mission Cross Bog	9	1110	4885	0.8	1.8	262	73	27.9	409	167
11	Ogaromtoc Lake	18	595	6166	3.0	2.9	423	283	66.9	1051	12
12	Patterson Lake	11	223	13,358	4.9	0.8	767	413	53.8	1655	49
14	Bluff Lake	11	431	14,606	2.6	0.8	947	336	35.5	1798	55
15	Twin Lake	10	410	16,042	2.4	0.6	933	719	77.1	3497	167
16	Fish Lake	31	671	3892	4.6	8.0	195	59	30.3	277	52
18	Mumbo Lake	6	267	14,426	2.2	0.4	1084	420	38.7	2083	58
19	Great Salt Lake	27	710	13,905	3.8	1.9	388	186	47.9	1495	172
21	Favre Lake	9	420	8038	2.1	1.1	569	226	39.7	893	6
22	Blue Lake Marsh	10	400	12,188	2.5	0.8	772	329	42.6	1575	176
27	Stonehouse Meadow	12	690	8787	1.7	1.4	465	197	42.4	871	**57**
28	Newark Valley Pond	6	100	5470	6.0	1.1	643	571	88.8	2112	145
29	Big Soda Lake	8	150	1548	5.3	5.2	199	86	43.2	358	50
32	Lily Pond	10	401	13,632	2.5	0.7	906	417	46.0	1729	189
33	Stella Lake	4	350	7399	1.1	0.5	603	190	31.5	922	176
34	Fallen Leaf Lake	14	987	11,623	1.4	1.2	482	145	30.1	783	209
37	Walker Lake	10	475	2718	2.1	3.7	312	259	83.0	993	39
39	Kirman Lake	9	310	9656	2.9	0.9	666	345	51.8	1369	28
40	Hidden Lake	9	500	14,880	1.8	0.6	855	268	31.3	1621	173
44	Mono Lake	22	352	10,351	6.3	2.1	620	344	55.5	1565	78
45	Glenmire	10	230	3244	4.3	3.1	146	83	56.8	370	27
46	Mono Lake	7	752	13,371	0.9	0.5	911	307	33.7	1687	251
48	Greenstone Lake	2	35	4095	5.7	0.5	1404	626	44.6	2762	471
50	Swamp Lake	14	947	19,687	1.5	0.7	745	311	41.7	1448	28
58	Starkweather Pond	3	30	3555	10.0	0.8	859	312	36.3	1792	338
60	Barrett Lake	4	60	5944	6.7	0.7	838	337	40.2	1620	322
63	Lower Pahranagat Lake	14	1240	5895	1.1	2.4	249	79	31.7	411	54
65	Skylark Pond	5	63	3193	7.9	1.6	430	291	67.7	1313	147
69	Owens Lake (OL84B)	24	812	14,072	3.0	1.7	524	156	29.8	822	251
72	Tulare Lake	22	440	20,121	5.0	1.1	702	343	48.9	1468	247
74	Zaca Lake	20	870	3074	2.3	6.5	152	70	46.1	318	40
75	Lower Bear Lake	23	400	9248	5.8	2.5	399	207	51.9	1026	90
76	Dry Lake	20	841	8753	2.4	2.3	289	136	47.1	790	142
78	Lake Elsinore	31	1074	9475	2.9	3.3	360	201	55.8	991	55
79	Soda Lake	6	1140	3853	0.5	1.6	494	88	17.8	625	270
80	Abbott Lake	10	560.5	2042	1.8	4.9	343	124	36.2	533	144
81	First Lake	23	456	11,588	5.04	2.0	458	223	48.7	1198	**77**
82	Second Lake	8	225	6330	3.56	1.3	552	320	58.0	1202	41
	mean	13	537	9281	3	2	572	261	46	1214	130

Table 3
Default Bacon parameters used for initial age-depth models.

Parameter	Default Value	Unit	Definition
d.min	uppermost date	cm	minimum depth of Bacon age model
d.max	lowermost date	cm	maximum depth of Bacon age model
thick	5	cm	Thickness of vertical sections core is divided into (starting from deepest to shallowest)
acc.mean	20	yr/cm	Mean time to accumulate 1 cm of sediment (mean value of the accumulation rate prior probability distribution)
acc.shape	1.5	unitless	Controls shape of the accumulation rate prior probability distribution. Larger vaules create a more peaked distribution.
mem.mean	0.7	unitless	Memory indicates dependence of accumulation rate on accumulation rate of previous section. mem.mean is the mean of the prior probability distribution for memory. Value ranges from 0 to 1, 0 = no memory, 1 = 100% memory
mem.strength	4	unitless	Controls shape of memory prior probablity distribution. Larger values create a more peaked distribution.
ssize	2000	iterations	The approximate number of iterations stored after the run

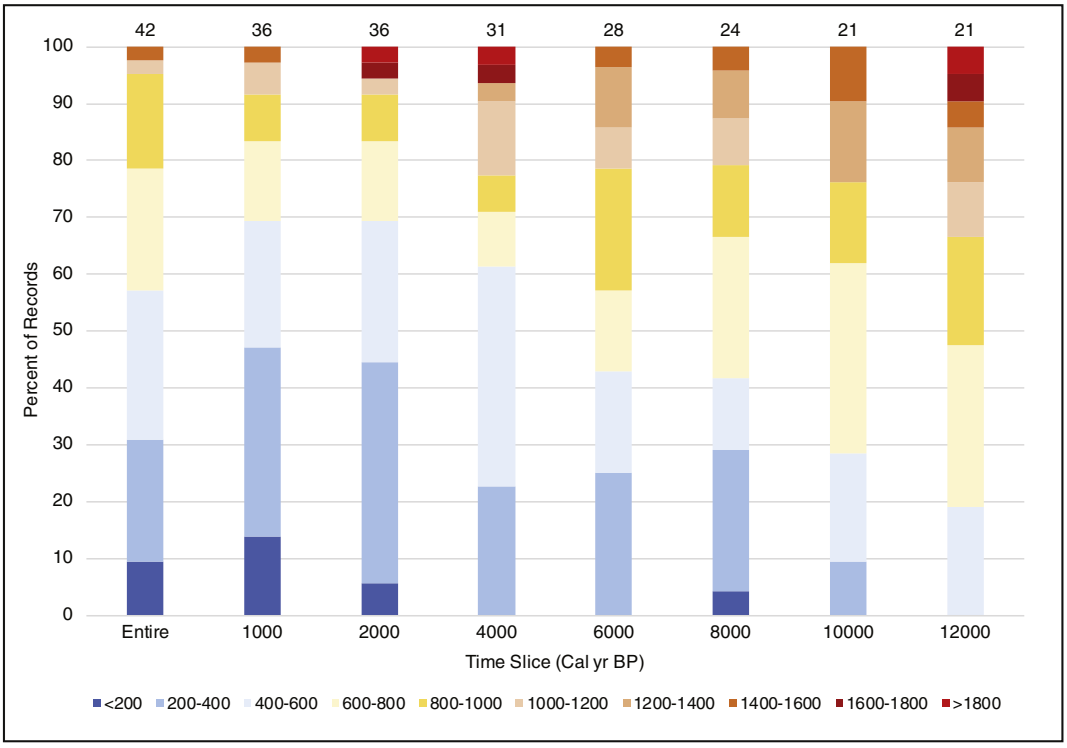

Fig. 4. The 95% uncertainty ranges of the Bacon age models, binned at 200 years, for the 42 sites examined in detail here. Columns show the mean uncertainties for entire age models (left column) and the uncertainties at specific moments at time (1 year) through the Holocene, expressed as percentage of age models considered for each time slice. The number of age models at each time is noted above the columns.

than 2 dates/kyr resulting in uncertainty greater than 400 years, no matter the temporal or physical length of the record. The amount of uncertainty in age models increases dramatically below that threshold, as does the scatter in the uncertainty; this corresponds directly to the finding of Blaauw et al. (2018) that a minimum of two dates per millennium is required to accurately capture the accumulation history of a core (e.g., Grimm, 2011). Fig. 6d shows that lower average deposition times (yr/cm) have lower uncertainties; this is likely due to the fact that cores with lower deposition times have higher dating densities. Based on these results, we strongly agree with the recommendation of Blaauw et al. (2018) that chronologies should be built in at least two phases, with no fewer than one date per millennium throughout to begin with, followed by additional dating targeted at intervals of interest and reaching a minimum of 2 dates/kyr.

There is a weak relationship between mean 95% uncertainty and the physical and temporal lengths of a core (Fig. 6e, 6f), with physically longer and temporally shorter records generally having lower uncertainty. The effect of physical length versus temporal length is illustrated by several records from the deglacial period. Greenstone Lake, Barrett Lake, and Starkweather Pond are quite short cores (30–60 cm) covering the deglacial period that have relatively high mean uncertainties (1404 yr, 838 yr, and 859 yr, respectively). The large uncertainties do not stem from the analytical uncertainty of the radiocarbon measurements (40–80 years); rather, they result from a small number of dates per kyr. The sediment sequences are 3500–6000 years long, and have only 2 to 4 dates each. In contrast, the deglacial record from Soda Lake core 24 (Honke et al., 2019) covers 3800 years in >10 m of core with 6 dates, and has a mean uncertainty of 494 years. In spite of the low number of dates per meter in the Soda Lake core, the larger number of dates per kyr produces a smaller uncertainty range. These findings highlight the prime importance of the length of time in a core, rather than its physical length, in determining the number of age

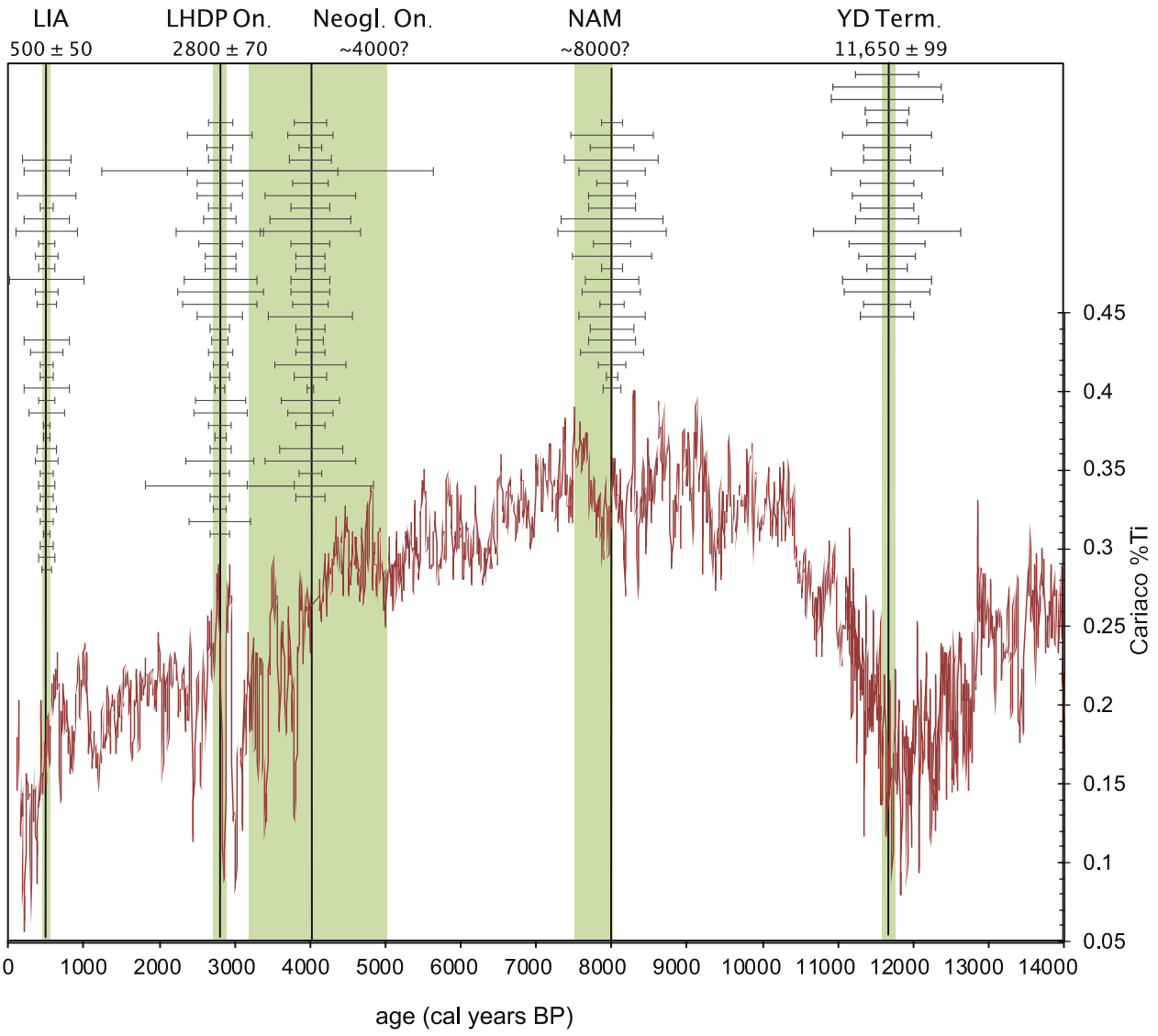

Fig. 5. Comparison of the 95% uncertainty ranges for the 42 age models with the paleoclimatic features expressed in the Cariaco Basin record of the Intertropical Convergence Zone (ITCZ), for the time slices of interest (see section 1.) Note that the width of green bars for the YD, LHDP, and LIA shows chronological uncertainties, while for the NAM and Neogl. it represents the range in age of climate proxy shifts in various records (as described for Fig. 2).

control points needed.

It appears that many investigators measure about 10 dates per record, regardless of the core length or the length of time being studied (Fig. 7): this suggests an artificial, probably budgetary, constraint. Although this is an unfortunate situation, the analysis presented here suggests that the budget required for work on a particular time period can be calculated at the proposal stage, without needing to know the physical length of the core(s) ahead of time. For example, to study the full Holocene (~12,000 yr) would require a minimum of 24 dates, regardless of the core length. Additional dates would be required if there were potential hiatuses or other irregularity in the cores, as well as for periods where additional chronological precision is required to make robust interpretations of the proxy data.

Examination of the down-core variability in uncertainty for each age model reveals several patterns and provides a framework for general approaches to initial dating of a core (Fig. 8). The first pattern, displayed by 18 of the age models, resembles the path of a bouncing ball, where the uncertainty increases between dates and is pulled back to a lower value at each date (Fig. 8a). In many cases, the uncertainty near the dates is quite regular, and the maximum uncertainty between dates is also similar. These tend to be records without significant changes in sediment type or accumulation rate, where sampling periodically in the depth dimension results in regular sampling in time also. The main control on the precision in these cases is the temporal gap between the dates: the farther apart the dates are (which frequently occurs in the bottom part of a core), the lower the precision; the closer the dates are in time, the better the precision.

The second clear pattern, displayed by 13 of the age models, shows a peak in uncertainty where there is a significant temporal gap between ages ("gap/peak" uncertainty, the "age-spacing problem" of Lacourse and Gajewski (2020); Fig. 8b). These gaps are readily apparent in the distribution of ages when plotted on a depth scale; however, how much the uncertainty increases in the gap is related to the time factor, with larger gaps in time producing a larger uncertainty. This is illustrated by the two dating gaps in Fig. 8b, where the 57 cm gap (131.5 cm−188.5 cm) produces a much

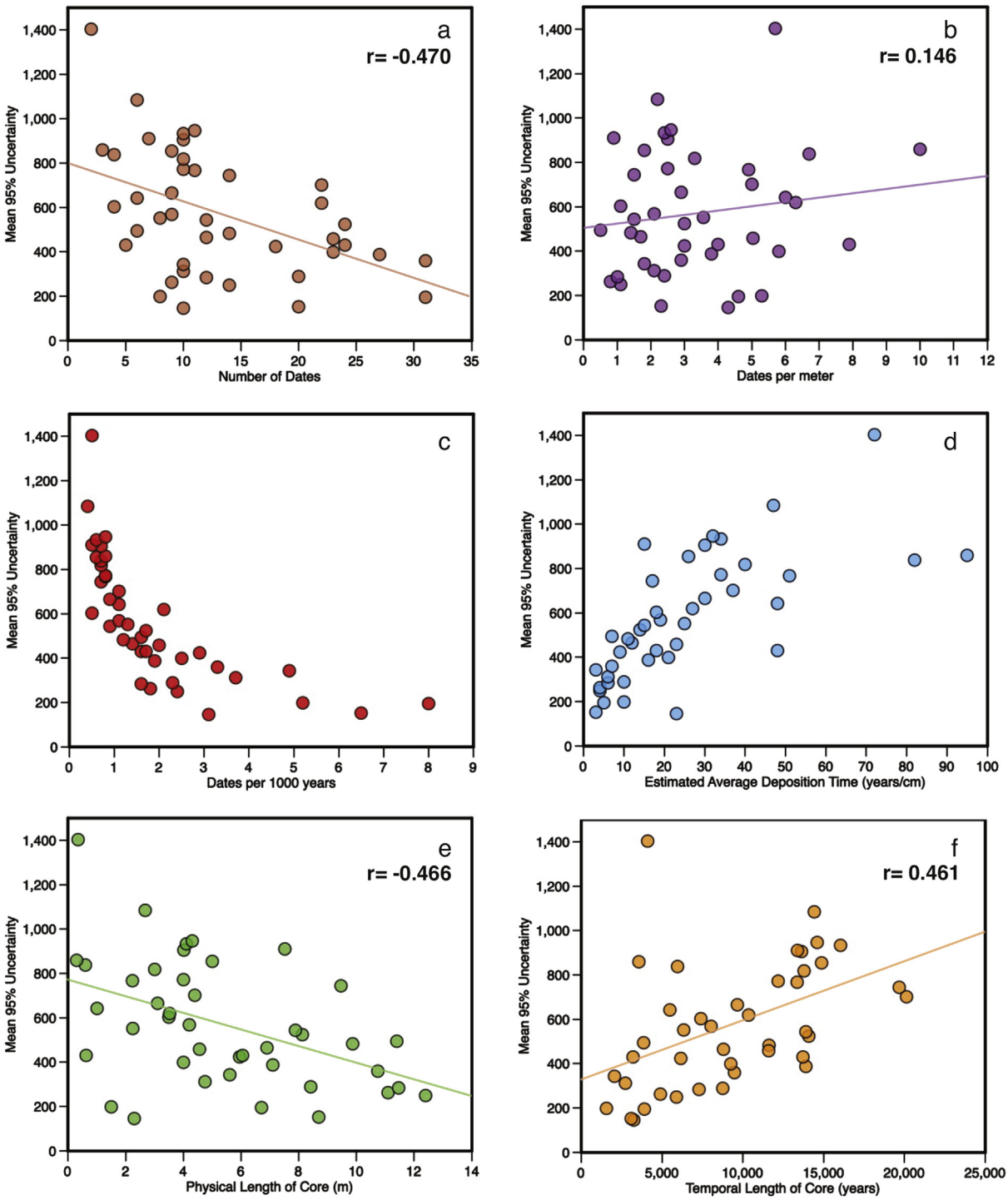

Fig. 6. Cross-plots showing the relationships between the mean 95% uncertainty of each age model with a) total number of dates in each record; b) number of dates per meter of core; c) number of dates per 1000 years; d) average deposition time (yr/cm); e) physical length of the core; and f) temporal length of the core.

larger increase in uncertainty than the 125.5 cm gap below it (194.5–320 cm); the temporal gaps are 3120 yr and 2500 yr, respectively, with sedimentation rates of 18 cm/kyr and 50 cm/kyr. Frequently the uncertainty of the age model is much better than that indicated by the mean, because of the excessive influence of the high uncertainty in gaps.

An additional pattern seen in a number of records is the expansion of the uncertainty associated with the oldest part of the record, because the paleoenvironmental information has been extrapolated below the oldest date (Fig. 8c). Extrapolating an age model so that paleoenvironmental interpretations can be made in spite of poor age control (e.g., Fig. 8b and c) is a dangerous excursion into unknown territory (Blaauw and Christen, 2013). In the 16 cases where the proxy records were extrapolated below the lowest date (from 8 to 130 cm, 118–1516 yr), the uncertainty at the base of the record was 1.4–5.3 times the uncertainty at the lowest date. In these cases, there is no apparent relationship between the number of centimeters of extrapolation and the increase in uncertainty.

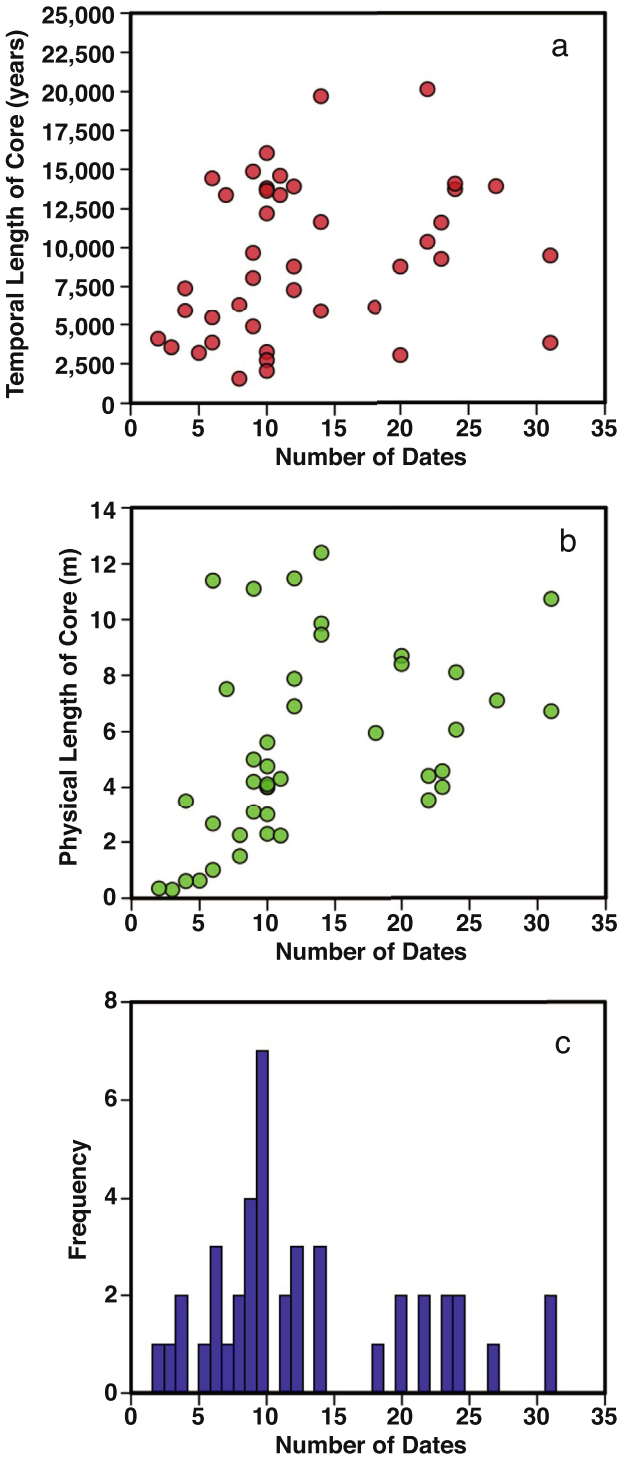

Fig. 7. Comparison of the number of dates in each age model with: a) temporal length of core (years) and b) the physical length of core (m). Panel c shows the overall distribution of the number of dates.

Rather, the size of the 95% uncertainty envelope at the base of the core is most closely related to the number of years of extrapolation. When proxy data interpretations are made in sections with extrapolated ages, it is prudent for the authors to alert the readers that this is the case (as in Street et al., 2012). Recognition of all of these phenomena during initial chronology construction should allow iterative rounds of dating to eliminate peak uncertainties, if suitable material for dating can be found.

5.3. Accuracy: geological uncertainty

Thus far, we have focused on the precision of the age models that can be constructed for the records. However, it is very important to note that no age modeling software can assess the accuracy of the underlying dates. Although most workers are aware of the potential for terrestrial macrofossils to be older than the sediment around them (e.g. charcoal or wood from the interior of a long-lived tree, deposition of "pre-aged" charcoal, robust seeds, or wood as discussed in section 2.1), ages affected by these processes can't be easily identified with very few dates, reinforcing the need for a minimum of two dates per millennium. The potential for bulk sediment to be distinctly too old is more problematic and more difficult to assess than for macrofossils, but in some settings there is simply no alternative to dating bulk-sediment carbon: no macrofossils can be found.

The advent of AMS dating, with its smaller sample-size requirement, significantly alleviated the uncertainty associated with dating the large sections of core required for decay-counting radiocarbon dating. Caution is still warranted, because the carbon being measured in a bulk-sediment sample still has an unknown source or mixture of sources, which can change over time. However, AMS also provides the opportunity for dating a combination of small macrofossils and bulk sediment to look for a potential reservoir effect, as well as dating individual components of bulk sediment, such as leaf waxes (i.e., compound-specific radiocarbon analysis), and pollen separates. These sources of additional information should be investigated if possible, but several studies show potential complications to simple interpretation of radiocarbon content (Howarth et al., 2013; Gierga et al., 2016; Zimmerman et al., 2018), and these must be assessed for each lake system. We have included records partially or wholly constructed of AMS dating of the carbon preserved in bulk sediment in our modeled records: of the 42 records, 7 are wholly reliant on bulk-sediment measurements, and 7 use a mixture of bulk-sediment and macrofossil ages.

In the Lower Pahranagat Lake age model (Fig. 9a), contribution of old carbon from springs was a clear possibility, as the study area is underlain by carbonate bedrock (Theissen et al., 2019). The authors suggested that bulk sediment and even some aquatic plants might be affected, yielding dates that were too old. Comparison of plant material and bulk sediment at the top of the core suggested a 590-year correction for old carbon, so this correction was applied to all of the bulk-sediment dates. In addition, a sample-specific $\delta^{13}C$ value was measured for each sample, and two plant macrofossils with anomalously heavy $\delta^{13}C$ values were also corrected. Terrestrial plant material from a C_3 pathway has an average $\delta^{13}C$ of around −28‰, while material from C_4 plants averages around −14‰ (Meyers and Lallier-Verges, 1999). The two suspicious macrofossils at Lower Pahranagat Lake were −8.9 and −15.3‰, which suggests that either they were aquatic plants that incorporated carbon from the lake water or that they came from a C_4 land plant such as saltbush (*Atriplex*).

At Stonehouse Meadow, Mensing et al. (2013) obtained a modern radiocarbon age on surface sediment, consistent with the observation that the springs feeding the meadow flow through shallow alluvial aquifers on 1- to 4-year timescales (indicated by tritium-helium dating of the water). A bulk-sediment sample gave the same age as a plant macrofossil at 390 cm, while a bulk-sediment date at 626.5 cm was about 500 years younger than a snail shell at the same level. One possible explanation is the identification of the snail as genus *Vallonia*, one of the genera that Pigati et al. (2010) suggested may incorporate radiocarbon-dead carbon

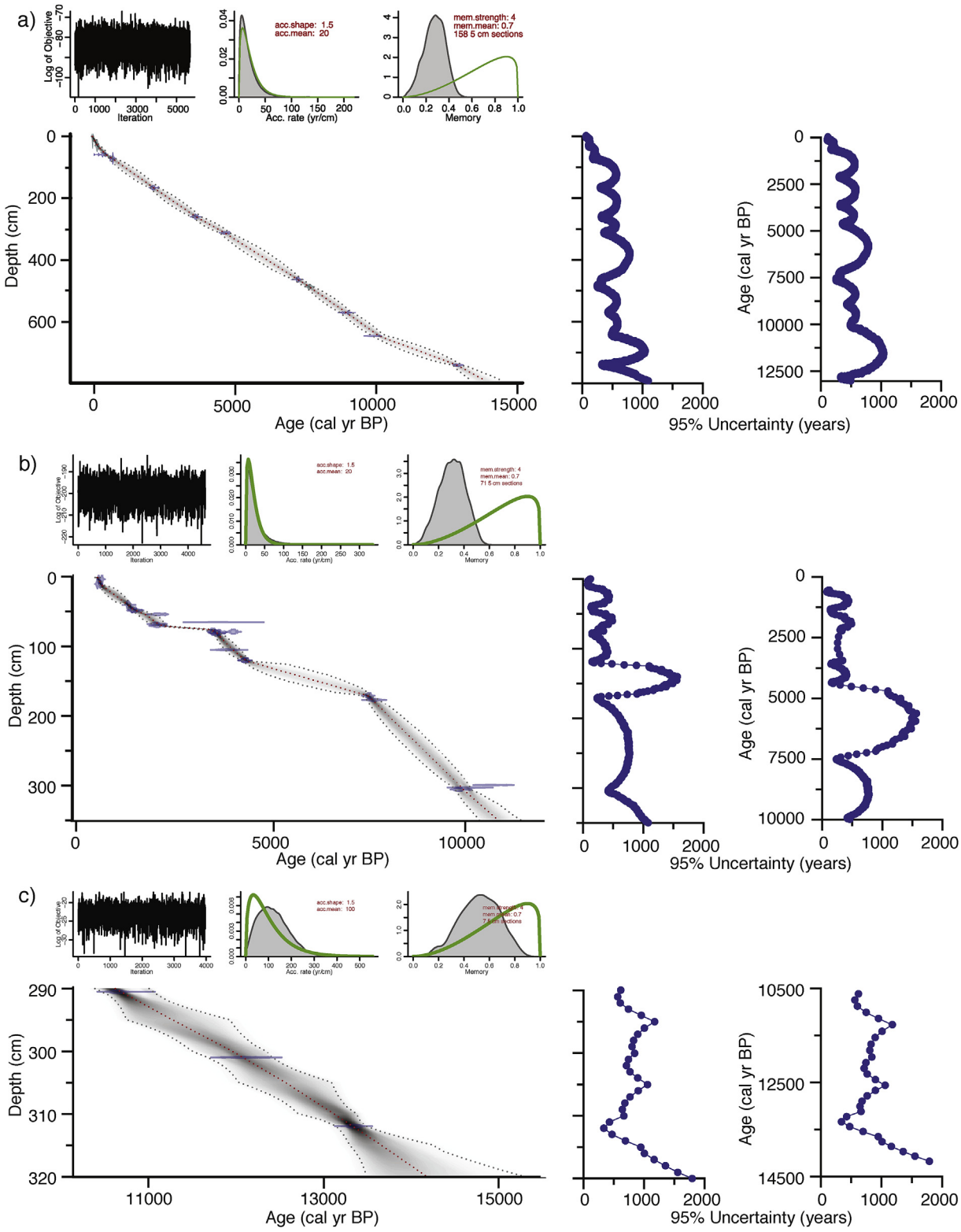

Fig. 8. Examples of Bacon age-depth plots (left column), showing typical patterns of down-core uncertainty, along with down-core 95% uncertainty ranges plotted on depth (center column) and age (right column). A) Bolan Lake (Briles et al., 2008) shows the typical bouncing-ball pattern that characterizes sites with relatively steady accumulation rates; b) Mono Lake (Zimmerman et al., accepted) shows a typical gap/peak uncertainty between 119 and 170 cm, where a gap between dates allows the uncertainty to expand significantly; and c) Starkweather Pond (MacDonald et al., 2008) shows the effect of too few dates per kyr and the typical expansion of uncertainty due to extrapolation below the oldest date.

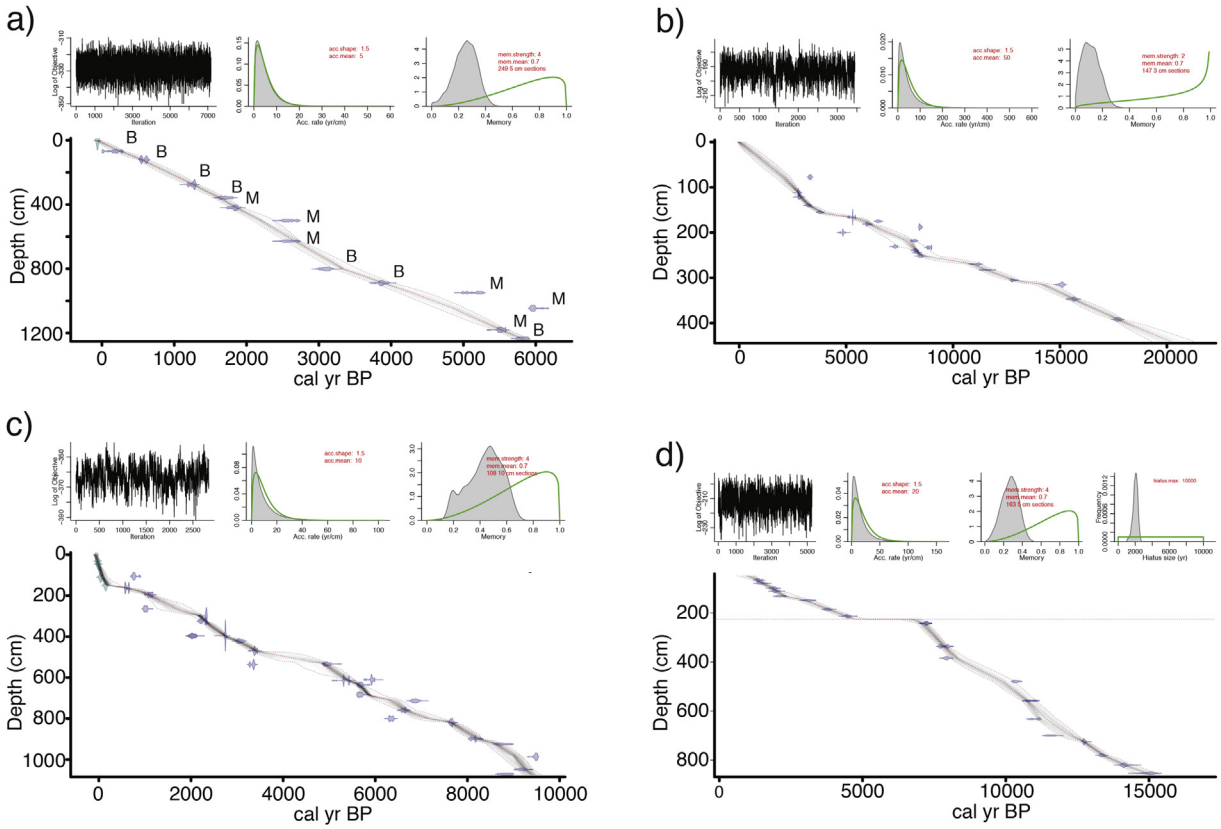

Fig. 9. Examples of Bacon plots from records dated primarily or exclusively with bulk-sediment AMS dates: a) Lower Pahranagat Lake (B = bulk, M = macrofossil); b) Tulare Lake; c) Lake Elsinore; d) Owens Lake.

into their shells if it is available. This may indicate that the bulk sediment date is in fact more reliable than the snail date.

Davis (1999a) rejected the only bulk-sediment measurement in his Mono Lake core, based on a pollen concentrate at the same depth which yielded a younger age; no sample preparation was given, and the sample was measured by decay counting. Bulk sediment and a cone scale at 540 cm in the Sanger Lake core (Briles et al., 2008) returned identical dates, suggesting that bulk-sediment dates should be reliable, although the oldest of the bulk-sediment dates (at 623 cm) was significantly older and was rejected. Three records mixed macrofossil and bulk-sediment dates with no attempt to test the bulk-sediment dates, at Barrett (2 of 4 dates) and Starkweather (1 of 3 dates) Lakes (MacDonald et al., 2008), and Hidden Lake (3 of 8 dates) (Potito et al., 2006).

Of the seven records that are almost entirely limited to bulk-sediment dates, only those for Lake Elsinore (Kirby et al., 2010) and Great Salt Lake (Thompson et al., 2016) explicitly describe the chemical treatment used to prepare the samples. In both cases all samples were acid washed, leaving only organic carbon. Thompson et al. (2016) described in detail the method used (10% HCl at 70 °C for 2–4 h) and noted that some samples also had Acid-Alkali-Acid treatment (giving a similar level of detail), with good agreement between methods. The extensive work on Great Salt Lake cores over the years (see especially references in Section 11.2.1 of Thompson et al., 2016) enabled assessment of organic carbon ages in the context of distinctive, well-established stratigraphy, a single wood date, and the Mazama and Hansel Valley tephras.

At Newark Valley and Kirman Lake, the authors described the samples as "bulk organic" but did not give any preparation description (Mensing et al., 2006; MacDonald et al., 2016); similarly at Greenstone Lake, no sample preparation was noted but the application of HCl to the samples indicated a lack of carbonate carbon (Porinchu et al., 2003). The Kirman Lake dates were not inconsistent with the Tsyowata tephra identified at ~248 cm. At Tulare Lake, no mention of the sample preparation methods is made, but Blunt and Negrini (2015) discuss the possibility of an old-carbon effect from re-worked organic carbon. The cores analyzed were taken within 100 m of a trench where a freshwater *Anodonta* shell produced the same age as bulk sediment at the same level, suggesting no reservoir effect. However, the ages for Tulare Lake cores are very scattered, indicating additional complexity of either carbon cycling or stratigraphy (Fig. 9b).

Ages measured on acid-washed bulk sediments from cores in Lake Elsinore also exhibit significant scatter (Fig. 9c). The upper part of the record is well-constrained from ^{210}Pb and exotic pollen correlated from a short core, but no correction was made to dates measured on LEGC03-2 and −3 (Kirby et al., 2010). A later study of the deglacial and older section used three macrofossil/bulk-sediment pairs and found a reservoir effect of approximately 915 years (Kirby et al., 2013), but the stability of that age offset through time and into the Holocene section is unknown.

Benson et al. (1997) used core OL84B (Fig. 9d) to reconstruct changes between 15.8 and 6.7 kyr in the Owens Lake basin, and the same core was used by Mensing (2001) to reconstruct pollen assemblages and by Bradbury and Forester (2002) to examine diatom and ostracod variations in Owens Lake. Benson et al. (1997) reported only that the age model for the OL84B core was based on 25 AMS ^{14}C dates on bulk organic carbon, but did not include a table of the dates (not uncommon at that time). Mensing (2001) included a table of dates, and noted the possibility that a reservoir correction up to 600 years may be needed, but didn't apply any correction. The OL84B dates are reported in the NCEI database (updated 8/2014),

and include a 600-year reservoir correction; these are the dates used for this study.

5.4. Holocene climate shifts in western U.S. Records

For the 42 records examined in detail here, we also analyzed the age precision of zone/event boundaries from the Younger Dryas to the present. These are boundaries that were identified by the original authors based on changes in the proxy data, as described in section 5.1.

The mean 95% uncertainty range for all 190 boundaries is 515 years, similar to the mean for age models as a whole, though with greater variability (standard deviation is 407 years, or 79%). Fig. 10 suggests a relationship (albeit weak) between the age of a boundary and uncertainty, with younger boundaries having lower uncertainties. This may be a result of temporally short records having a similar number of dates per record as longer records (Fig. 7a), resulting in increased dating density (more dates per kyr). Nearly half of the boundaries (n = 91, 47.9%) have an uncertainty range <400 years (Fig. 11), which is reasonably precise for multi-centennial-scale reconstructions. Of the 20 boundaries with uncertainty ranges less than 100 years, 14 of them are from the sediment surface, 11 of which come from sites that have age control above the youngest radiocarbon age (i.e., ^{210}Pb, exotic pollen, etc). These results highlight the importance of using dating techniques to control the age of the youngest sediment, as these sections are critical for calibrating proxy data to the instrumental record.

The majority of boundary uncertainties are greater than 400 years, with 66 boundaries (34.7%) falling between 400 and 800 years and 33 boundaries (17.4%) greater than 800 years (Fig. 11). These large uncertainties greatly reduce the confidence in knowing when a particular change in proxy data occurred. Many of the largest uncertainties result from issues that were identified above, associated with either large gaps in age control or from ages extrapolated below the lowest radiocarbon date. The 21 boundaries that have uncertainties greater than 1000 years come from 10 sites, 9 of which suffered from gap/peak issues and 1 of which was associated with extrapolated ages. The most striking feature of this analysis is that most of the gap/peak sites had relatively good age control overall, but gaps in dating of just 2000 years easily resulted in uncertainties greater than 1000 years. Larger gaps compounded the problem, with several zone/event boundaries falling within a single gap. The Newark Valley age model (Mensing et al., 2006) highlights this issue, with four boundaries that exhibit uncertainties between 1670 and 2110 years all falling within one 3500-year age control gap.

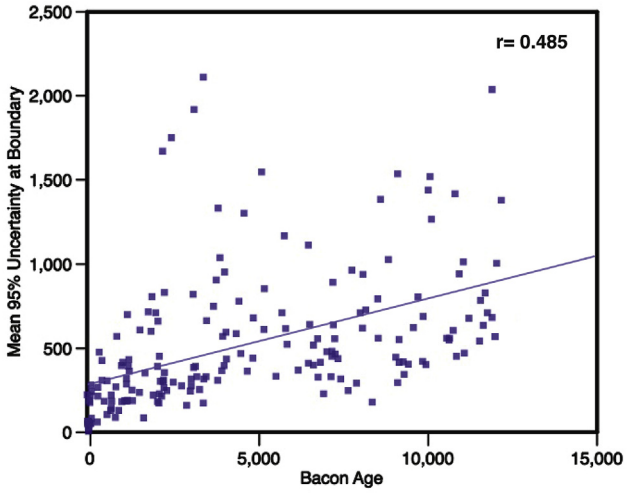

Fig. 10. Comparison of the 95% uncertainty at each zone/event boundary identified in the records examined with the age of the boundary from the new Bacon model.

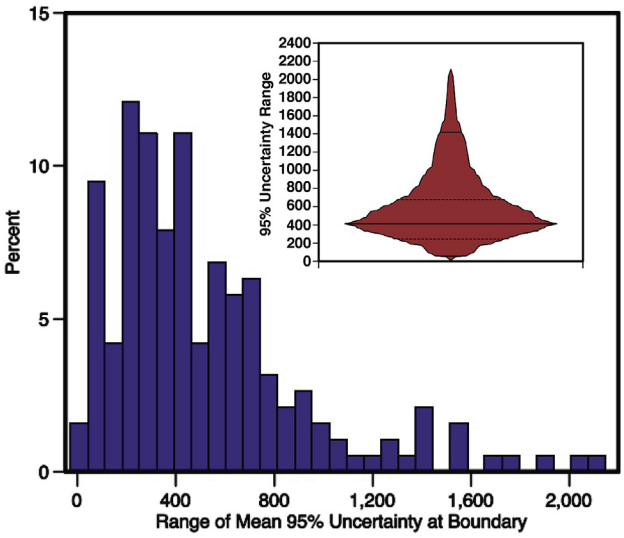

Fig. 11. Percent distribution of 95% uncertainty values at zone/event boundaries: inset shows percentile box with distribution shape.

We also looked at the zone/event boundaries as they relate to the five time slices described in section 1 (Fig. 12). Of the 21 sites that record the period of the transition from the Younger Dryas to the Early Holocene, 8 have zone/event boundaries (n = 9) whose 95% uncertainty range overlaps with 11,650 cal yr BP.

The smallest 95% uncertainty window on any of the shifts is > 540 years and the average is > 950 years, making it impossible to determine if any of the changes noted is correlative with, for example, the shifts associated with the end of the Younger Dryas in North Pacific proxy data (Hendy et al., 2002; Praetorius and Mix, 2014), or in the Greenland ice sheet (Rasmussen et al., 2006). Further obscuring the situation, one of the sites notes two environmental changes that occurred sequentially, that each have uncertainty envelopes that overlap the Younger Dryas boundary. In that record, the question of which shift is the response (if either, in fact) to the large, abrupt change seen in the global system can't be answered definitively.

Evaluation of the western US response to the hypothesized organization of the modern North American monsoon system (Barron et al., 2012) is complicated by the fact that the timing of the reorganization itself is not well defined. The conceptual model presented by Barron et al. (2012) generally suggests a broader area of more diffuse monsoon rainfall before about 8000 years ago, with the modern core of more intense but spatially restricted rainfall developing by 6000 years ago. This pattern suggests testable predictions for the records examined here: for example, records in southern California and Nevada should show a contribution of tropical Pacific moisture before ~8000 years ago, probably making the sites wetter than after ~8000 years ago, while eastern Great Basin sites might be drier before ~8000 years ago, until the larger contribution of monsoon moisture began by the Middle Holocene. Without better constraints on the timing of the development of the monsoon system, we can note only that of the 23 sites that span that period, 7 sites have 8 boundaries whose age precisely overlaps 8000 cal yr BP (Fig. 12): with one exception, these boundaries have uncertainties ranging from 620 to 1385 years.

The shift from warmer, drier Middle Holocene conditions to

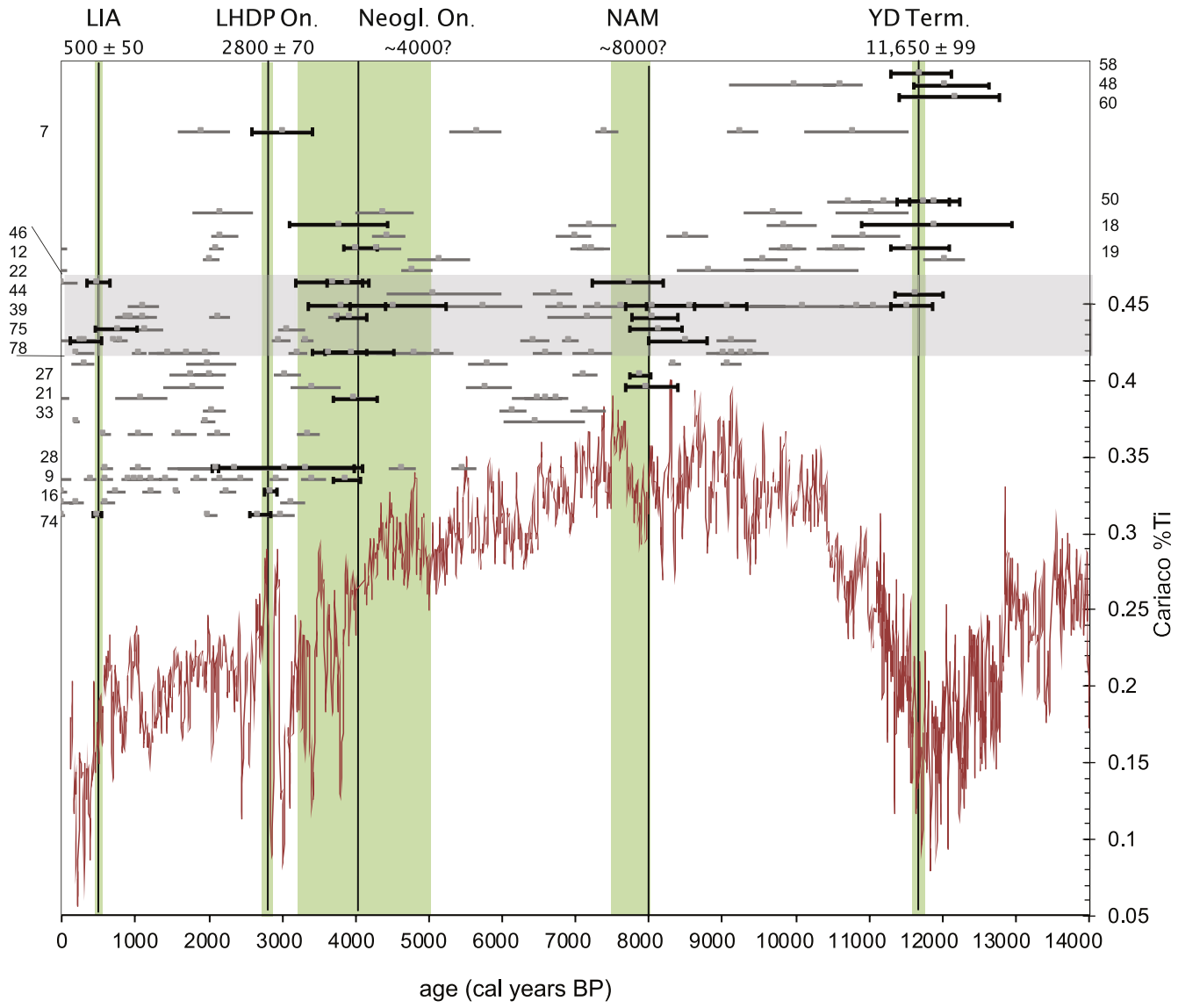

Fig. 12. Illustration of the overlap between the ages of the zone/event boundaries in each record and the times of major paleoclimate change in the western United States. Pink curve below is the Cariaco Basin record of the ITCZ, and the green bands are as described for Fig. 2. Boundaries whose age-uncertainty window overlaps the year of the shift are shown in black; corresponding site numbers from Table 1 are listed on the y axes. Gray bars indicate boundaries that do not overlap temporally with the single year; some do overlap with the green uncertainty boxes (see section 6 for discussion). Many of these may be local changes in environment or ecology, but a pattern of changes overlapping the major climate shifts would indicate a larger-scale driver of regional change. Note that not all of the boundaries identified are shown, as some are younger than 1950 CE (0 cal yr BP).

colder and wetter Late Holocene conditions at about 4000 years ago is well documented (Neoglacial), and evidence is increasing for an extreme drought beginning at about 2800 years ago (Late Holocene Dry Period). However, these two events are generally not distinguishable in the records examined here, due to uncertainties that are large relative to the time between the climate shifts. In fact, at two sites an environmental shift is recorded whose uncertainty allows it to be attributed to either period (Fig. 12). Although it could be argued that any indication of a shift to colder wetter conditions around this time must be correlative with the onset of the Neoglacial, and evidence for aridity with the Late Holocene Dry Period, reliance on such assumptions prevents the development of robust spatial maps of either event. For example, Mensing et al. (2013) described a dipole pattern in the records of the Late Holocene Dry Period that they examined, with a shift to wetter conditions in the northwest: such a regional map requires that the conditions mapped are constrained within a fairly restricted interval of time, something that is currently impossible to do with the existing chronologies.

The period of the transition from the Medieval Climate Anomaly to the Little Ice Age at about 500 years ago (e.g., Stine, 1990) is recorded by nearly all the sites, but remarkably few have distinct proxy shifts at that time (Fig. 12). This may be in part because of native peoples managing the landscape for food and other resources, especially in California. Although the intentional use of fire has been recognized for decades, the extent to which the regional vegetation (and thus the pollen rain to lakes and meadows) was affected has not been clear (Cowart and Byrne, 2013). We find that few pollen records of the last 1000 years examined here have been interpreted through an anthropogenic lens. A notable exception to this is Crawford et al. (2015), whose research design included comparison of proxy data from Fish and Ogaromtoc Lakes, located near archaeological sites, with higher-elevation paleoclimate records remote from human activities to separate the potential

impact of Native American land use from purely climatic changes.

Analysis of the uncertainties associated with zone/event boundaries show that many changes observed in proxy data lack the needed precision for comparison with other records. In each climate shift except the Neoglacial onset, there are between 2 and 7 additional sites with zone/event boundaries whose age uncertainty overlaps the uncertainty on the age of the shift. An improvement in the age precision, or a change in the actual age of the shift, might significantly change the patterns of correlation. This is especially true for the Neoglacial onset, where, in addition to the 9 sites with 11 boundaries overlapping 4000 cal yr BP, there are another 18 records with zone boundaries that overlap the current range of 5000 to 3200 cal yr BP. Additional work to assess the environmental changes and age uncertainties of glacial, lacustrine, marine, and other records of that period is needed to define spatial and temporal patterns of proxy signals.

When authors compare changes in their data with those reported in multiple records across a region without considering all of the uncertainties, the relationships posited between proxy data can be tenuous or misleading. This is particularly true when attempting to determine leads/lags between sites or to assess spatial patterns of change. Authors traditionally deal with these uncertainties by describing the timing of changes with qualifying words such as "around" or "approximately" (e.g., around 3500 cal yr BP or ~3500 cal yr BP), without consideration of whether the uncertainty permits a unique correlation between sites. Instead, we recommend that proxy shifts be discussed using both age and uncertainty, to clearly demonstrate the precision of the timing (Zimmerman et al., accepted). In addition, any discussion of the timing of changes from multiple sites requires knowledge and careful consideration of the uncertainties in *each* record being considered, including the uncertainties on age models for widely cited canonical records.

6. Conclusions and recommendations

Based on the analysis presented here, many of the existing records of terrestrial environmental conditions in the western United States are not suitable for studies of sub-millennial climate change during the Holocene. This includes several well-cited studies and is due to insufficient dating. For sites initially studied in the 1970's, '80's, and early '90's, this is due in part to the constraints imposed by decay counting, but also because many were developed in order to understand broad patterns of post-glacial change. However, a number of these sites show great promise for addressing modern questions about past and future climate that require higher-resolution sampling, and would benefit from the application of modern techniques.

The widespread use of AMS for measurement of ^{14}C samples revolutionized the situations in which radiocarbon dating could be applied, as well as the time required for measurement (days vs. weeks). In enabling dating of small macrofossils rather than bulk sediment, the resolution and accuracy of the age models was also generally improved. In spite of this, even many of the existing records with reliable age models have mean uncertainties of >500 years, due to gaps in dating where uncertainty is 1000 years or greater. The zone/event boundaries exhibit even less precision, with 50% having uncertainties of >500 and 15.6% greater than 1000 years.

The strongest predictor of low uncertainty in age models is the number of dates per millennium, regardless of the physical or temporal length of the core. This means that shorter cores do not necessarily require fewer dates if they have a slow sediment accumulation rate, but also that physically longer cores, which can yield high-resolution proxy data, do not necessarily need more dates.

We suggest that an iterative dating approach such as that described by Blaauw et al. (2018) will be the most successful at producing the highest precision chronology. Examination of a new core should thus begin with 2–3 "range-finder" dates spread throughout the core, focusing especially on the top- and bottom-most useable sections. With the number of years covered by the core determined from these dates, the minimum number needed to reach 2 dates per kyr can be calculated. This approach also suggests that the minimum number of dates necessary for a study can be calculated in advance (i.e., at the proposal stage) based on the anticipated period of time being studied and the temporal resolution needed. Along with adequate dating density, both the precision and accuracy of age models can be improved by taking multiple cores to ensure complete recovery, using multiple methods of age control whenever possible (e.g, tephras, non-native pollen, ^{210}Pb in addition to radiocarbon), and carefully assessing the upper section of the core to ensure the sediment/water interface was captured with minimal disturbance.

In addition to age-model precision, the accuracy of ages is paramount. Terrestrial materials, especially relatively fragile macrofossils such as leaves or other annual plant material, are most preferred. In cases where bulk-sediment dates cannot be avoided, the chemical preparation should include at least an acid wash and (as always) should be described in the methods. The thickness of the samples should also be reported, as it is critical to assessing the precision of the resulting age. Radiocarbon measurement of the surface sediment and/or the lake or spring water(s) can check for the current contribution of radiocarbon-depleted carbon to the system. Terrestrial macrofossils or charcoal should be dated when found, with a paired sample of bulk sediment at the same depth to monitor for a change in the contribution of old water through time, if measurement of bulk-sediment ^{14}C will be used anywhere in the core. This is especially important for long records that may have been subject to very different climatic and hydrologic conditions at times in the past. Measurement of a sample-specific $\delta^{13}C$ value is recommended whenever the sample size permits (for both bulk sediment and unidentified macrofossils). Identification of macrofossil material is extremely useful when the possibility of aquatic or partially submergent vegetation exists, and good guides can be found if a plant expert is not readily at hand (e.g., Marty and Myrbo, 2014). Finally, uncertainty in the accuracy of bulk-sediment ages must be considered in correlation of proxy data, especially where those ages show noticeable scatter.

Use of a Bayesian approach for constructing an age model is made relatively simple with Bacon (Blaauw and Christen, 2011) and other freely available computer programs, and the calculation of uncertainty for every depth in a core can help identify locations in a core where an additional date or two will make the most impact. In the presentation of the proxy data, the practice of plotting age control points along with the proxy records is a simple way to demonstrate the quality of the age control for the record.

This review provides a critical, quantitative analysis of chronologic control and uncertainties associated with age models constructed for paleoclimate studies from the western U.S. Our findings show that age model uncertainties are relatively large when compared to several Holocene climate shifts. These uncertainties not only preclude the ability to confidently compare datasets to canonical paleoclimate records such as those from Greenland and the Cariaco Basin, they highlight the imprecision underlying any effort to correlate datasets from different sites. We find that although large uncertainties currently prevent sub-centennial interpretations in most cases, increased dating density, strategic use of limited funds (including budgeting for a 2 date/kyr minimum at the proposal stage), construction of age-depth models with

Bayesian methods, and critical evaluation of chronological uncertainty will shed light on past climate variability at finer timescales, enhancing our understanding of global and regional drivers of western U.S. climate.

Author statement

Susan Zimmerman and David Wahl: Conceptualization, Methodology, Formal analysis, Investigation, Writing - original draft, Writing - review & editing, Visualization.

Data availability

Bacon parameters for all new models created here are available in SI Table 1; Bacon age-depth plots and bouncing-ball uncertainty plots for those models are in SI Fig. 1. No other new data was generated for this study.

Declaration of competing interest

The authors declare that they have no known competing financial interests or personal relationships that could have appeared to influence the work reported in this paper.

Acknowledgments

This work was supported by the USGS Climate and Land Use Research and Development Program and grant LDRD-17-ERD-052 from LLNL to SRHZ. The manuscript was greatly improved by thoughtful comments from J. Rodysill and three anonymous reviewers. We thank M. Champagne for help with Table 3. The leave granted by LLNL to SRHZ and the warm hospitality of the faculty, students, and staff of The Institute for Earth Sciences of The Hebrew University of Jerusalem are gratefully acknowledged. This is LLNL-JRNL-807185.

References

Adam, D.P., 1967. Late-Pleistocene and recent palynology in the central Sierra Nevada. In: Cushing, E.J., Wright, H.E.J. (Eds.), Quaternary Paleoecology: New Haven, Conn. Yale University Press, pp. 275–301.

Adam, D.P., 1975. A late Holocene pollen record from Pearson's Pond, Weeks Creek landslide, San Francisco peninsula, California: U.S. Geol. J. Res. 3 (6), 721–731.

Adam, D.P., 1988. Correlations of the Clear Lake, California, core CL-73-4 pollen sequence with other long climate records. In: Sims, J.D. (Ed.), Late Quaternary Climate, Tectonism, and Sedimentation in Clear Lake, Northern California Coast Ranges: Boulder. Geological Society of America, pp. 81–95.

Adam, D.P., Byrne, R., Luther, E., 1981a. A late Pleistocene and Holocene pollen record from Laguna de las Trancas, northern coastal Santa Cruz County, California. Madroño 28 (4), 255–272.

Adam, D.P., Sims, J.D., Throckmorton, C.K., 1981b. 130,000-yr continuous pollen record from Clear Lake, Lake County, California. Geology 9 (8), 373.

Adams, K.D., 2003. Age and paleoclimatic significance of late Holocene lakes in the Carson Sink. NV, USA: Quat. Res. 60, 294–306.

Adams, K.D., Rhodes, E.J., 2019. Late Holocene paleohydrology of Walker Lake and the Carson Sink in the western Great Basin. Nevada, USA: Quaternary Research, pp. 1–18.

Allan, M., 2003. A 2000 Year Record of Vegetation and Climate Change in the Jarbridge Mountains of Northeastern Nevada [M.S. Thesis]. University of Nevada, Reno, p. 65.

Alley, R.B., 2000. The Younger Dryas cold interval as viewed from central Greenland. Quat. Sci. Rev. 19, 213–226.

Anderson, R.S., 1987. Late-Quaternary Environments of the Sierra Nevada. California [Ph.D. thesis]. University of Arizona, p. 290.

Anderson, R.S., 1990. Holocene forest development and paleoclimates within the central Sierra Nevada, California. J. Ecol. 78 (2), 470–489.

Anderson, R.S., 2005. Contrasting Vegetation and Fire Histories on the Point Reyes Peninsula during the Pre-settlement and Settlement Periods: 15,000 Years of Change.

Anderson, R.S., Byrd, B.F., 1998. Late-Holocene vegetation changes from the Las Flores Creek coastal lowlands, San Diego County, California. Madroño 45 (2), 171–182.

Anderson, R.S., Davis, O.K., 1988. Contemporary pollen rain across the central Sierra Nevada, California, U.S.A.: Relationship to modern vegetation types. Arct. Alp. Res. 20 (4), 448–460.

Anderson, R.S., Davis, O.K., Fall, P.L., 1985. Late glacial and Holocene vegetation and climate in the Sierra Nevada of California, with particular reference to the Balsam Meadow site. In: Jacobs, B.F., Fall, P.L., Davis, O.K. (Eds.), Late Quaternary Vegetation and Climates of the American Southwest, American Association of Stratigraphic Palynologists, pp. 127–140.

Anderson, R.S., Ejarque, A., Brown, P.M., Hallett, D.J., 2013. Holocene and historical vegetation change and fire history on the north-central coast of California. USA: Holocene 23 (12), 1797–1810.

Anderson, R.S., Smith, S.J., Jass, R.M., Spaulding, W.G., 2008. A late Holocene record of vegetation and climate from a small wetland in Shasta County. California: Madrono 55 (1), 15–25.

Antinao, J.L., McDonald, E., Rhodes, E.J., Brown, N., Barrera, W., Gosse, J.C., Zimmerman, S., 2016. Late Pleistocene-Holocene alluvial stratigraphy of southern Baja California. Mexico: Quat. Sci. Rev. 146, 161–181.

Appleby, P.G., 1998. Dating Recent Sediments by 210Pb: Problems and Solutions. International Atomic Energy Agency.

Appleby, P.G., Oldfield, F., Thompson, R., Huttunen, P., Tolonen, K., 1979. 210Pb dating of annually laminated lake sediments from Finland. Nature 280 (5717), 53–55.

Aquino-Lopez, M.A., Blaauw, M., Christen, J.A., Sanderson, N.K., 2018. Bayesian analysis of 210Pb dating. Journal of Agricultural, Biological, and Environmental Statistics.

Atwater, B.F., Adam, D.P., Bradbury, J.P., Forester, R.M., Mark, R.K., Lettis, W.R., Fisher, G.R., Gobalet, K.W., Robinson, S.W., 1986. A fan dam for Tulare Lake, California, and implications for the Wisconsin glacial history of the Sierra Nevada. Geol. Soc. Am. Bull. 97, 97–109.

Bacon, S.N., Burke, R.M., Pezzopane, S.K., Jayko, A.S., 2006. Last glacial maximum and Holocene lake levels of Owens Lake, eastern California. USA: Quat. Sci. Rev. 25, 1264–1282.

Ball, G.I., Noble, P.J., Stephens, B.M., Higgins, A., Mensing, S.A., Aluwihare, L.I., 2019. A lignin, diatom, and pollen record spanning the Pleistocene–Holocene transition at Fallen Leaf Lake, Sierra Nevada, California, USA. In: Starratt, S.W., Rosen, M.R. (Eds.), From Saline to Freshwater: the Diversity of Western Lakes in Space and Time. Geological Society of America Special. Paper 536.

Barron, J.A., Heusser, L.E., Alexander, C., 2004. High resolution climate of the past 3,500 years of coastal northernmost California. In: Starratt, S.W., Blomquist, N.L. (Eds.), Twentieth Annual Pacific Climate Workshop: Pacific Grove, CA, State of California. Dept. of Water Resources, pp. 13–22.

Barron, J.A., Metcalfe, S.E., Addison, J.A., 2012. Response of the North American monsoon to regional changes in ocean surface temperature. Paleoceanography 27, 3.

Barsanti, M., Garcia-Tenorio, R., Schirone, A., Rozmaric, M., Ruiz-Fernández, A.C., Sanchez-Cabeza, J.A., Delbono, I., Conte, F., De Oliveira Godoy, J.M., Heijnis, H., Eriksson, M., Hatje, V., Laissaoui, A., Nguyen, H.Q., Okuku, E., Al-Rousan, S.A., Uddin, S., Yii, M.W., Osvath, I., 2020. Challenges and limitations of the 210Pb sediment dating method: Results from an IAEA modelling interlaboratory comparison exercise. Quat. Geochronol. 59.

Bartlein, P.J., Edwards, M.E., Shafer, S.L., Barker, E.D., 1995. Calibration of radiocarbon ages and the interpretation of paleoenvironmental records. Quat. Res. 44, 417–424.

Bartlein, P.J., Harrison, S.P., Brewer, S., Connor, S., Davis, B.A.S., Gajewski, K., Guiot, J., Harrison-Prentice, T.I., Henderson, A., Peyron, O., Prentice, I.C., Scholze, M., Seppä, H., Shuman, B., Sugita, S., Thompson, R.S., Viau, A.E., Williams, J., Wu, H., 2010. Pollen-based continental climate reconstructions at 6 and 21 ka: a global synthesis. Clim. Dynam. 37 (3–4), 775–802.

Beaty, R.M., Taylor, A.H., 2009. A 14 000 year sedimentary charcoal record of fire from the northern Sierra Nevada, Lake Tahoe Basin. California, USA: Holocene 19 (3), 347–358.

Bennett, C.L., Beukins, R.P., Clover, M.R., Gove, H.E., Liebert, R.B., Litherland, A.E., Purser, K.H., Sondheim, W.E., 1977. Radiocarbon dating using electrostatic accelerators: Negative ions provide the key. Science 198, 508–510.

Benson, L., Burdett, J., Lund, S., Kashgarian, M., Mensing, S., 1997. Nearly synchronous climate change in the Northern Hemisphere during the last glacial termination. Nature 388, 263–265.

Benson, L., Kashgarian, M., Rye, R., Lund, S., Paillet, F., Smoot, J., Kester, C., Mensing, S., Meko, D., Lindstrom, S., 2002. Holocene multidecadal and multicentennial droughts affecting Northern California and Nevada. Quat. Sci. Rev. 21, 659–682.

Benson, L.V., Burdett, J.W., Kashgarian, M., Lund, S.P., Phillips, F.M., Rye, R.O., 1996. Climatic and hydrologic oscillations in the Owens Lake basin and adjacent Sierra Nevada. California: Science 274, 746–749.

Benson, L.V., Meyers, P.A., Spencer, R.J., 1991. Change in the size of Walker Lake during the past 5000 years. Palaeogeogr. Palaeoclimatol. Palaeoecol. 81, 189–214.

Bird, B.W., Kirby, M.E., 2006. An Alpine Lacustrine Record of Early Holocene North American Monsoon Dynamics from Dry Lake, Southern California (USA).

J. Paleolimnol. 35 (1), 179–192.
Bird, B.W., Kirby, M.E., Howat, I.M., Tulaczyk, S., 2010. Geophysical evidence for Holocene lake-level change in southern California (Dry Lake). Boreas 39 (1), 131–144.
Blaauw, M., Christen, J.A., 2011. Flexible paleoclimate age-depth models using an autoregressive gamma process. Bayesian Analysis 6 (3), 457–474.
Blaauw, M., Christen, J.A., 2013. Bacon Manual. https://CRAN.R-project.org/package=rbacon p. 15.
Blaauw, M., Christen, J.A., Bennett, K.D., Reimer, P.J., 2018. Double the dates and go for Bayes - Impacts of model choice, dating density and quality on chronologies. Quat. Sci. Rev. 188, 58–66.
Blunt, A.B., Negrini, R.M., 2015. Lake levels for the past 19,000 years from the TL05-4 cores, Tulare Lake, California, USA: Geophysical and geochemical proxies. Quat. Int. 387, 122–130.
Bowerman, N.D., Clark, D.H., 2011. Holocene glaciation of the central Sierra Nevada, California. Quat. Sci. Rev. 30, 1067–1085.
Bradbury, J.P., Forester, R.M., 2002. Environment and paleolimnology of Owens Lake, California: A record of climate and hydrology for the last 50,000 years. In: Hershler, R., Madsen, D.B., Currey, D.R. (Eds.), Great Basin Aquatic Systems History, Smithsonian, pp. 145–173.
Bradbury, J.P., Forester, R.M., Thompson, R.S., 1989. Late Quaternary paleolimnology of Walker Lake, Nevada. J. Paleolimnol. 1, 249–267.
Bright, R.C., 1966. Pollen and seed stratigraphy of Swan Lake, southeastern Idaho: Tebiwa. Journal of the Idaho State University Museum 9 (2), 1–47.
Briles, C.E., 2008. Holocene Vegetation and Fire History of the Floristically Diverse Klamath Mountains, Northern California, USA [Ph.D. Thesis]. University of Oregon, p. 227.
Briles, C.E., Whitlock, C., Bartlein, P.J., 2005. Postglacial vegetation, fire, and climate history of the Siskiyou Mountains, Oregon. USA: Quat. Res. 64 (1), 44–56.
Briles, C.E., Whitlock, C., Bartlein, P.J., Higuera, P., 2008. Regional and local controls on postglacial vegetation and fire in the Siskiyou Mountains, northern California. USA: Palaeogeogr. Palaeoclimatol. Palaeoecol. 265 (1–2), 159–169.
Broecker, W.S., Walton, A.F., 1959. The geochemistry of ^{14}C in freshwater systems. Geochemica et Cosmochemica Acta 16, 15–38.
Bronk Ramsey, C., 1995. Radiocarbon calibration and analysis of stratigraphy: The OxCal program. Radiocarbon 37 (2), 425–430.
Bronk Ramsey, C., 2008. Radiocarbon Dating: Revolutions in Understanding. Archaeometry 50 (2), 249–275.
Bronk Ramsey, C., 2009. Bayesian analysis of radiocarbon dates. Radiocarbon 51 (1), 337–360.
Bronk Ramsey, C., Lee, S., 2013. Recent and planned developments of the program OxCal. Radiocarbon 55 (2–3), 720–730.
Brunelle, A., Anderson, R.S., 2003. Sedimentary charcoal as an indicator of late-Holocene drought in the Sierra Nevada, California, and its relevance to the future. Holocene 13 (1), 21–28.
Bursik, M., Reid, J., 2004. Lahar in Glass Creek and Owens River during the Inyo eruption, Mono–Inyo Craters, California. J. Volcanol. Geoth. Res. 131 (3–4), 321–331.
Bursik, M., Sieh, K., 2013. Digital Database of the Holocene Tephras of the Mono-Inyo Craters, vol. 758. U.S. Geological Survey Data Series, California.
Bursik, M., Sieh, K., Meltzner, A., 2014. Deposits of the most recent eruption in the Southern Mono Craters, California: Description, interpretation and implications for regional marker tephras. J. Volcanol. Geoth. Res. 275, 114–131.
Carpenter, S.L., 1991. Vegetation change in Yosemite Valley, Yosemite National Park, California, during the protohistoric period. Madroño 38 (1), 1–13.
Chen, Y., Smith, P.E., Evensen, N.M., York, D., Lajoie, K.R., 1996. The Edge of Time: Dating Young Volcanic Ash Layers with the ^{40}Ar-^{39}Ar Laser Probe. Science 274, 1176–1178.
Cole, K.L., Liu, G.-w., 1994. Holocene paleoecology of an estuary on Santa Rosa Island, California. Quat. Res. 41, 326–335.
Colman, S.M., Rosenbaum, J.G., Kaufman, D.S., Dean, W.E., McGeehin, J.P., 2009. Radiocarbon Ages and Age Models for the Past 30,000 Years in Bear Lake, Utah and Idaho, Paleoenvironments of Bear Lake, Utah and Idaho, and its Catchment.
Cowart, A., Byrne, R., 2013. A Paleolimnological Record of Late Holocene Vegetation Change from the Central California Coast. Calif. Archaeol. 5 (2), 337–352.
Cox, S.E., Farley, K.A., Hemming, S.R., 2012. Insights into the age of the Mono Lake Excursion and magmatic crystal residence time from (U-Th)/He and ^{230}Th dating of volcanic allanite. Earth Planet Sci. Lett. 319–320, 178–184.
Crawford, J.N., Mensing, S.A., Lake, F.K., Zimmerman, S.R., 2015. Late Holocene fire and vegetation reconstruction from the western Klamath Mountains, California, USA: A multi-disciplinary approach for examining potential human land-use impacts. Holocene 25 (8), 1341–1357.
Damon, P.E., Lerman, J.C., Long, A., 1978. Temporal fluctuations of atmospheric ^{14}C: causal factors and implications. Annu. Rev. Earth Planet Sci. 6, 457–494.
Daniels, M.L., Anderson, R.S., Whitlock, C., 2005. Vegetation and fire history since the Late Pleistocene from the Trinity Mountains, northwestern California. USA: Holocene 15 (7), 1062–1071.
Dansgaard, W., Johnsen, S.J., Clausen, H.B., Dahl-Jensen, D., Gundestrup, N.S., Hammer, C.U., Hvidberg, C.S., Steffensen, J.P., Sveinbjornsdottir, A.E., Jouzel, J., Bond, G., 1993. Evidence for general instability of past climate from a 250-kyr ice-core record. Nature 364, 218–220.
Davis, J.O., 1977. Quaternary Tephrochronology of the Lake Lahontan Area, Nevada and California [Ph.D. Thesis]. University of Idaho, p. 150.
Davis, O.K., 1999a. Pollen analysis of a Late-Glacial and Holocene sediment core from Mono Lake, Mono County, California. Quat. Res. 52, 243–249.
Davis, O.K., 1999b. Pollen analysis of Tulare lake, California: Great Basin-like vegetation in Central California during the full-glacial and early Holocene. Rev. Palaeobot. Palynol. 107, 249–257.
Davis, O.K., Anderson, R.S., Fall, P.L., O'Rourke, M.K., Thompson, R.S., 1985. Palynological evidence for early Holocene aridity in the southern Sierra Nevada. California: Quat. Res. 24, 322–332.
Davis, O.K., Moratto, M.J., 1988. Evidence for a warm dry early Holocene in the western Sierra Nevada of California: Pollen and plant macrofossil analysis of Dinkey and Exchequer Meadows. Madroño 35 (2), 132–149.
Davis, P.T., Menounos, B., Osborn, G., 2009. Holocene and latest Pleistocene alpine glacier fluctuations: a global perspective. Quat. Sci. Rev. 28, 2012–2033.
Deevey, E.S., Gross, M.S., Hutchinson, G.E., Kraybill, H.L., 1954. The natural 14C contents of materials from hard-water lakes. Proc. Natl. Acad. Sci. U. S. A. 40, 285–288.
De Vries, H., 1958. Variations in concentration of radiocarbon with time and location on Earth. Koninkl Ned. Akad. Wetensch. Prodc. B61, 94–102.
Dingemans, T., Mensing, S.A., Feakins, S.J., Kirby, M.E., Zimmerman, S.R.H., 2014. 3000 years of environmental change at Zaca Lake, California. USA: Frontiers in Ecology and Evolution 2.
Drexler, J.Z., Fuller, C.C., Archfield, S., 2018. The approaching obsolescence of ^{137}Cs dating of wetland soils in North America. Quat. Sci. Rev. 199, 83–96.
Edlund, E.G., Byrne, R., 1991. Climate, Fire and Late Quaternary Vegetation Change in the Central Sierra Nevada. USDA Forest Service.
Egan, J., Staff, R., Blackford, J., 2015. A high-precision age estimate of the Holocene Plinian eruption of Mount Mazama. Oregon, USA: Holocene 25 (7), 1054–1067.
Enzel, Yehouda, Brown, William J., Anderson, Roger Y., McFadden, Leslie D., Wells, Stephen G., 1992. Short-duration Holocene lakes in the Mojave River drainage basin, southern California. Quaternary Research 38, 60–73.
Enzel, Y., Cayan, D.R., Anderson, R.Y., Wells, S.G., 1989. Atmospheric circulation during Holocene lake stands in the Mojave Desert: evidence of regional climate change. Nature 341, 44–47.
Feakins, S.J., Kirby, M.E., Cheetham, M.I., Ibarra, Y., Zimmerman, S.R.H., 2014. Fluctuation in leaf wax D/H ratio from a southern California lake records significant variability in isotopes in precipitation during the late Holocene. Org. Geochem. 66, 48–59.
Foit, F.F.J., Mehringer Jr., P.J., 2016. Holocene tephra stratigraphy in four lakes in southeastern Oregon and northwestern Nevada. USA: Quat. Res. 85, 218–226.
Fritz, S.C., Metcalfe, S.E., Dean, W., 2001. Holocene climate patterns in the Americas inferred from paleolimnological records. In: Markgraf, V. (Ed.), Interhemispheric Climate Linkages. Academic Press, pp. 241–263.
Gierga, M., Hajdas, I., van Raden, U.J., Gilli, A., Wacker, L., Sturm, M., Bernasconi, S.M., Smittenberg, R.H., 2016. Long-stored soil carbon released by prehistoric land use: Evidence from compound-specific radiocarbon analysis on Soppensee lake sediments. Quat. Sci. Rev. 144, 123–131.
Godwin, H., 1962. Half-life of radiocarbon. Nature 195, 984.
Grimm, E.C., 2011. High-resolution age model based on AMS radiocarbon ages for Kettle Lake, North Dakota. USA: Radiocarbon 53 (1), 39–53.
Grootes, P.M., Stuiver, M., 1997. Oxygen 18/16 variability in Greenland snow and ice with 10^3 to 10^5-year time resolution. J. Geophys. Res. 102, 26455–26470.
Hallett, D.J., Anderson, R.S., 2010. Paleofire reconstruction for high-elevation forests in the Sierra Nevada, California, with implications for wildfire synchrony and climate variability in the late Holocene. Quat. Res. 73, 180–190.
Harrison, S.P., Kutzbach, J.E., Liu, Z., Bartlein, P.J., Otto-Bliesner, B., Muhs, D., Prentice, I.C., Thompson, R.S., 2003. Mid-Holocene climates of the Americas: a dynamical response to changed seasonality. Clim. Dynam. 20 (7–8), 663–688.
Haslett, J., Parnell, A.C., 2008. A simple monotone process with application to radiocarbon-dated depth chronologies. J. Roy. Stat. Soc. 57, 399–418.
Haug, G.H., Hughen, K.A., Sigman, D.M., Peterson, L.C., Rohl, U., 2001. Southward migration of the Intertropical Convergence Zone through the Holocene. Science 293, 1304–1308.
Hendy, I.L., Kennett, J.P., Roark, E.B., Ingram, B.L., 2002. Apparent synchroneity of submillennial scale climate events between Greenland and Santa Barbara Basin, California from 30-10 ka. Quat. Sci. Rev. 21, 1167–1184.
Hermann, N.W., Oster, J.L., Ibarra, D.E., 2018. Spatial patterns and driving mechanisms of mid-Holocene hydroclimate in western North America. J. Quat. Sci. 33 (4), 421–434.
Heusser, L.E., Hendy, I.L., Barron, J.A., 2015. Vegetation response to southern California drought during the Medieval Climate Anomaly and early Little Ice Age (AD 800–1600). Quat. Int. 387, 23–35.
Hiner, C.A., Kirby, M.E., Bonuso, N., Patterson, W.P., Palermo, J., Silveira, E., 2016. Late Holocene hydroclimatic variability linked to Pacific forcing: evidence from Abbott Lake, coastal central California. J. Paleolimnol. 56, 299–313.
Hogg, A., Fifield, L., Turney, C., Palmer, J., Galbraith, R., Baillie, M., 2006. Dating ancient wood by high-sensitivity liquid scintillation counting and accelerator mass spectrometry—Pushing the boundaries. Quat. Geochronol. 1 (4), 241–248.
Honke, J.S., Pigati, J.S., Wilson, J., Bright, J., Goldstein, H.L., Skipp, G.L., Reheis, M.C., Havens, J.C., 2019. Late Quaternary paleohydrology of desert wetlands and pluvial lakes in the Soda Lake basin, central Mojave Desert, California (USA). Quat. Sci. Rev. 216, 89–106.
Howarth, J.D., Fitzsimons, S.J., Jacobsen, G.E., Vandergoes, M.J., Norris, R.J., 2013. Identifying a reliable target fraction for radiocarbon dating sedimentary records from lakes. Quat. Geochronol. 17, 68–80.
Hua, Q., 2009. Radiocarbon: A chronological tool for the recent past. Quat. Geochronol. 4 (5), 378–390.
Hua, Q., Barbetti, M., Rakowski, A.Z., 2013. Atmospheric radiocarbon for the period

1950-2010. Radiocarbon 55 (4), 2059–2072.
Hughen, K., Lehman, S., Southon, J., Overpeck, J., Marchal, O., Herring, C., Turnbull, J., 2004. ^{14}C Activity and Global Carbon Cycle Changes over the Past 50,000 Years. Science 303, 202–207.
Hughen, K., Southon, J., Lehman, S., Bertrand, C., Turnbull, J., 2006. Marine-derived ^{14}C calibration and activity record for the past 50,000 years updated from the Cariaco Basin. Quat. Sci. Rev. 25 (23–24), 3216–3227.
John, D.A., duBray, E.A., Blakely, R.J., Fleck, R.J., Vikre, P.G., Box, S.E., Moring, B.C., 2012. Miocene magmatism in the Bodie Hills volcanic field, California and Nevada: A long-lived eruptive center in the southern segment of the ancestral Cascades arc. Geosphere 8 (1), 44–97.
Kent, D.V., Hemming, S.R., Turrin, B.D., 2002. Laschamp Excursion at Mono Lake? Earth and Planetary Science Letters 197, 151–164.
Kirby, M.E., Feakins, S.J., Bonuso, N., Fantozzi, J.M., Hiner, C.A., 2013. Latest Pleistocene to Holocene hydroclimates from Lake Elsinore, California. Quat. Sci. Rev. 76, 1–15.
Kirby, M.E., Feakins, S.J., Hiner, C.A., Fantozzi, J., Zimmerman, S.R.H., Dingemans, T., Mensing, S.A., 2014. Tropical Pacific forcing of Late-Holocene hydrologic variability in the coastal southwest United States. Quat. Sci. Rev. 102, 27–38.
Kirby, M.E., Knell, E.J., Anderson, W.T., Lachniet, M.S., Palermo, J., Eeg, H., Lucero, R., Murrieta, R., Arevalo, A., Silveira, E., Hiner, C.A., 2015. Evidence for insolation and Pacific forcing of late glacial through Holocene climate in the Central Mojave Desert (Silver Lake, CA). Quat. Res. 84 (2), 174–186.
Kirby, M.E., Lund, S.P., Anderson, M.A., Bird, B.W., 2007. Insolation forcing of Holocene climate change in Southern California: a sediment study from Lake Elsinore. J. Paleolimnol. 38 (3), 395–417.
Kirby, M.E., Lund, S.P., Patterson, W.P., Anderson, M.A., Bird, B.W., Ivanovici, L., Monarrez, P., Nielsen, S., 2010. A Holocene record of Pacific Decadal Oscillation (PDO)-related hydrologic variability in Southern California (Lake Elsinore, CA). J. Paleolimnol. 44 (3), 819–839.
Kirby, M.E., Lund, S.P., Poulsen, C.J., 2005. Hydrologic variability and the onset of modern El Niño-Southern Oscillation: a 19 250-year record from Lake Elsinore, southern California. J. Quat. Sci. 20 (3), 239–254.
Kirby, M.E.C., Patterson, W.P., Lachniet, M., Noblet, J.A., Anderson, M.A., Nichols, K., Avila, J., 2019b. Pacific Southwest United States Holocene Droughts and Pluvials Inferred From Sediment δ18O(calcite) and Grain Size Data (Lake Elsinore, California). Front. Earth Sci. 7.
Kirby, M.E., Poulsen, C.J., Lund, S.P., Patterson, W.P., Reidy, L., Hammond, D.E., 2004. Late Holocene lake level dynamics inferred from magnetic susceptibility and stable oxygen isotope data: Lake Elsinore, southern California (USA). J. Paleolimnol. 31, 275–293.
Kirby, M.E., Zimmerman, S.R.H., Patterson, W.P., Rivera, J.J., 2012. A 9170-year record of decadal-to-multi-centennial scale pluvial episodes from the coastal Southwest United States: a role for atmospheric rivers? Quat. Sci. Rev. 46, 57–65.
Kirby, M.E., Patterson, W.P., Ivanovici, L., Sandquist, D., Glover, K.C., 2019a. Evidence for a Large Middle Holocene Flood Event in the Pacific Southwestern United States (Lake Elsinore, California), from Saline to Freshwater: the Diversity of Western Lakes in Space and Time. Geological Society of America.
Klein, J., Lerman, J.C., Damon, P.E., Ralph, E.K., 1982. Calibration of radiocarbon dates: Tables based on the consensus data of the Workshop on Calibrating the Radiocarbon Time Scale. Radiocarbon 24 (2), 103–150.
Knott, J.R., Machette, M.N., Wan, E., Klinger, R.E., Liddicoat, J.C., Sarna-Wojcicki, A.M., Fleck, R.J., Deino, A.L., Geissman, J.W., Slate, J.L., Wahl, D.B., Wernicke, B.P., Wells, S.G., Tinsley, J.C., Hathaway, J.C., Weamer, V.M., 2018. Late Neogene–Quaternary tephrochronology, stratigraphy, and paleoclimate of Death Valley. California, USA: GSA Bulletin 130 (7–8), 1231–1255.
Koehler, P.A., Anderson, R.S., 1994. The paleoecology and stratigraphy of Nichols Meadow, Sierra National Forest. California, USA: Palaeogeogr. Palaeoclimatol. Palaeoecol. 112, 1–17.
Kohfeld, K.E., Harrison, S.P., 2000. How well can we simulate past climates? Evaluating the models using global palaeoenvironmental datasets. Quat. Sci. Rev. 19, 321–346.
Lacourse, T., Gajewski, K., 2020. Current practices in building and reporting age-depth models. Quat. Res. 96, 28–38.
Li, H.-C., Bischoff, J.L., Ku, T.-L., Lund, S.P., Stott, L.D., 2000. Climate Variability in East-Central California during the Past 1000 Years Reflected by High-Resolution Geochemical and Isotopic Records from Owens Lake Sediments. Quat. Res. 54, 189–197.
Louderback, L.A., Rhode, D.E., 2009. 15,000 years of vegetation change in the Bonneville basin: the Blue Lake pollen record. Quat. Sci. Rev. 28, 308–326.
Lowe, D.J., 2011. Tephrochronology and its application: A review. Quat. Geochronol. 6 (2), 107–153.
Lund, S.P., 1996. A comparison of Holocene paleomagnetic secular variation records from North America. J. Geophys. Res. 101 (B4), 8007–8024.
Lund, S.P., Platzman, E., 2015. Paleomagnetic chronostratigraphy of late Holocene Zaca Lake, California. Holocene 26 (5), 814–821.
MacDonald, G.M., Moser, K.A., Bloom, A.M., Porinchu, D.F., Potito, A.P., Wolfe, B.B., Edwards, T.W.D., Petel, A., Orme, A.R., Orme, A.J., 2008. Evidence of temperature depression and hydrological variations in the eastern Sierra Nevada during the Younger Dryas stade. Quat. Res. 70 (2), 131–140.
MacDonald, G.M., Moser, K.A., Bloom, A.M., Potito, A.P., Porinchu, D.F., Holmquist, J.R., Hughes, J., Kremenetski, K.V., 2016. Prolonged California aridity linked to climate warming and Pacific sea surface temperature. Sci. Rep. 6, 33325.
Marcaida, M., Mangan, M.T., Vazquez, J.A., Bursik, M., Lidzbarski, M.I., 2014. Geochemical fingerprinting of Wilson Creek formation tephra layers (Mono Basin, California) using titanomagnetite compositions. J. Volcanol. Geoth. Res. 273, 1–14.
Marcaida, M., Vazquez, J.A., Stelten, M.E., Miller, J.S., 2019. Constraining the Early Eruptive History of the Mono Craters Rhyolites, California, Based on ^{238}U-^{230}Th Isochron Dating of Their Explosive and Effusive Products: Geochemistry. Geophysics, Geosystems.
Marty, J., Myrbo, A., 2014. Radiocarbon dating suitability of aquatic plant macrofossils. J. Paleolimnol. 52 (4), 435–443.
Masson-Delmotte, V., Schulz, M., Abe-Ouchi, A., Beer, J., Ganopolski, A., González Rouco, J.F., Jansen, E., Lambeck, K., Luterbacher, J., Naish, T., Osborn, T., Otto-Bliesner, B., Quinn, T., Ramesh, R., Rojas, M., Shao, X., Timmermann, A., 2013. Information from Paleoclimate Archives. In: Stocker, T.F., Qin, D., Plattner, G.-K., Tignor, M., Allen, S.K., Boschung, J., Nauels, A., Xia, Y., Bex, V., Midgley, P.M. (Eds.), Climate Change 2013: the Physical Science Basis. Contribution of Working Group 1 to the Fifth Assessment Report of the Intergovernmental Panel on Climate Change. Cambridge University Press, Cambridge, UK and New York, NY, USA.
Mensing, S., Livingston, S., Barker, P., 2006. Long-term fire history in Great Basin sagebrush reconstructed from macroscopic charcoal in spring sediments, Newark Valley, Nevada. Western North American Naturalist 66 (1), 64–77.
Mensing, S., Smith, J., Burkle Norman, K., Allan, M., 2008. Extended drought in the Great Basin of western North America in the last two millennia reconstructed from pollen records. Quat. Int. 188 (1), 79–89.
Mensing, S., Southon, J., 1999. A simple method to separate pollen for AMS radiocarbon dating and its application to lacustrine and marine sediments. Radiocarbon 41 (1), 1–8.
Mensing, S.A., 2001. Late-Glacial and Early Holocene Vegetation and Climate Change near Owens Lake, Eastern California. Quat. Res. 55 (1), 57–65.
Mensing, S.A., Benson, L.V., Kashgarian, M., Lund, S., 2004. A Holocene pollen record of persistent droughts from Pyramid Lake, Nevada. USA: Quat. Res. 62, 29–38.
Mensing, S.A., Sharpe, S.E., Tunno, I., Sada, D.W., Thomas, J.M., Starratt, S., Smith, J., 2013. The Late Holocene Dry Period: multiproxy evidence for an extended drought between 2800 and 1850 cal yr BP across the central Great Basin. USA: Quat. Sci. Rev. 78, 266–282.
Metcalfe, S.E., Barron, J.A., Davies, S.J., 2015. The Holocene history of the North American Monsoon: 'known knowns' and 'known unknowns' in understanding its spatial and temporal complexity. Quat. Sci. Rev. 120, 1–27.
Meyers, P.A., Benson, L.V., 1988. Sedimentary biomarker and isotopic indicators of the paleoclimatic history of the Walker Lake basin, western Nevada. Org. Geochem. 13, 807–813.
Meyers, P.A., Lallier-Verges, E., 1999. Lacustrine sedimentary organic matter records of Late Quaternary paleoclimates. J. Paleolimnol. 21, 345–372.
Millar, C.I., King, J.C., Westfall, R.D., Alden, H.A., Delany, D.L., 2006. Late Holocene forest dynamics, volcanism, and climate change at Whitewing Mountain and San Joaquin Ridge, Mono County, Sierra Nevada. CA, USA: Quat. Res. 66, 273–287.
Miller, G.H., Geirsdóttir, Á., Zhong, Y., Larsen, D.J., Otto-Bliesner, B.L., Holland, M.M., Bailey, D.A., Refsnider, K.A., Lehman, S.J., Southon, J.R., Anderson, C., Björnsson, H., Thordarson, T., 2012. Abrupt onset of the Little Ice Age triggered by volcanism and sustained by sea-ice/ocean feedbacks. Geophys. Res. Lett. 39 (2) (n/a-n/a.).
Minckley, T.A., Whitlock, C., Bartlein, P.J., 2007. Vegetation, fire, and climate history of the northwestern Great Basin during the last 14,000 years. Quat. Sci. Rev. 26 (17–18), 2167–2184.
Mohr, J.A., Whitlock, C., Skinner, C.N., 2000. Postglacial vegetation and fire history, eastern Klamath Mountains, California. USA: Holocene 10 (5), 587–601.
Moser, K.A., Kimball, J.P., 2009. A 19,000-year Record of Hydrologic and Climatic Change Inferred from Diatoms from Bear Lake, Utah and Idaho, Paleoenvironments of Bear Lake, Utah and Idaho, and its Catchment.
Muller, R.A., 1977. Radioisotope dating with a cyclotron. Science 196 (4289), 489–494.
Negrini, R.M., Erbes, D.B., Faber, K., Herrera, A.M., Roberts, A.P., Cohen, A.S., Wigand, P.E., Franklin, F., Foit, J., 2000. A paleoclimate record for the past 250,000 years from Summer Lake, Oregon, USA: I. Chronology and magnetic proxies for lake level. J. Paleolimnol. 24, 125–149.
Negrini, R.M., Wigand, P.E., Draucker, S., Gobalet, K.W., Gardner, J.K., Sutton, M.Q., Yohe, R.M., 2006. The Rambla highstand shoreline and the Holocene lake-level history of Tulare Lake, California. USA: Quat. Sci. Rev. 25, 1599–1618.
Nelson, D.E., Korteling, R.G., Stott, W.R., 1977. Carbon-14: Direct detection at natural concentrations. Science 198, 507–508.
Newton, M.S., 1991. Holocene Stratigraphy and Magnetostratigraphy of Owens and Mono Lakes. University of Southern California, Ph.D. dissertation, Eastern California, p. 330.
Newton, M.S., 1994. Holocene Fluctuations of Mono Lake, California: the Sedimentary Record, Sedimentology and Geochemistry of Modern and Ancient Saline Lakes. SEPM (Society for Sedimentary Geology) Sp. Pub. No. 50, pp. 143–157.
Noble, P.J., Ball, G.I., Zimmerman, S.H., Maloney, J., Smith, S.B., Kent, G., Adams, K.D., Karlin, R.E., Driscoll, N., 2016. Holocene paleoclimate history of Fallen Leaf Lake, CA., from geochemistry and sedimentology of well-dated sediment cores. Quat. Sci. Rev. 131, 193–210.
Norman, K., 2007. A High Resolution Re-examination of Vegetation and Climate Change in the Jarbridge Mountains of Northeastern Nevada from 4,000 to 2000 Cal Yr BP [M.S. Thesis]. University of Nevada, Reno, p. 100.

Osleger, D.A., Heyvaert, A.C., Stoner, J.S., Verosub, K.L., 2008. Lacustrine turbidites as indicators of Holocene storminess and climate: Lake Tahoe, California and Nevada. J. Paleolimnol. 42 (1), 103–122.
Oster, J.L., Montañez, I.P., Sharp, W.D., Cooper, K.M., 2009. Late Pleistocene California droughts during deglaciation and Arctic warming. Earth Planet Sci. Lett. 288 (3–4), 434–443.
Owen, L.A., Finkel, R.C., Minnich, R.A., Perez, A.E., 2003. Extreme southwestern margin of late Quaternary glaciation in North America: Timing and controls. Geology 31 (8), 729–732.
Owen, L.A., Bright, J., Finkel, R.C., Jaiswal, M.K., Kaufman, D.S., Mahan, S., Radtke, U., Schneider, J.S., Sharp, W., Singhvi, A.K., Warren, C.N., 2007. Numerical dating of a Late Quaternary spit-shoreline complex at the northern end of Silver Lake playa, Mojave Desert, California: A comparison of the applicability of radiocarbon, luminescence, terrestrial cosmogenic nuclide, electron spin resonance, U-series and amino acid racemization methods. Quat. Int. 166 (1), 87–110.
Parnell, A.C., Buck, C.E., Doan, T.K., 2011. A review of statistical chronology models for high-resolution, proxy-based Holocene palaeoenvironmental reconstruction. Quat. Sci. Rev. 30, 2948–2960.
Pigati, J.S., Rech, J.A., Nekola, J.C., 2010. Radiocarbon dating of small terrestrial gastropod shells in North America. Quat. Geochronol. 5 (5), 519–532.
Plater, A.J., Boyle, J.F., Mayers, C., Turner, S.D., Stroud, R.W., 2006. Climate and human impact on lowland lake sedimentation in Central Coastal California: the record from c. 650 AD to the present. Reg. Environ. Change 6, 71–85.
Polyak, V.J., Rasmussen, J.B.T., Asmerom, Y., 2004. Prolonged wet period in the southwestern United States through the Younger. Dryas: Geology 32 (1), 5–8.
Porinchu, D.F., MacDonald, G.M., Bloom, A.M., Moser, K.A., 2003. Late Pleistocene and early Holocene climate and limnological changes in the Sierra Nevada, California, USA inferred from midges (Insecta: Diptera: Chironomidae). Palaeogeogr. Palaeoclimatol. Palaeoecol. 198 (3–4), 403–422.
Potito, A.P., Porinchu, D.F., MacDonald, G.M., Moser, K.A., 2006. A late Quaternary chironomid-inferred temperature record from the Sierra Nevada, California, with connections to northeast Pacific sea surface temperatures. Quat. Res. 66, 356–363.
Praetorius, S.K., Mix, A.C., 2014. Synchronization of North Pacific and Greenland climates preceded abrupt deglacial warming. Science 345 (6195), 444–448.
Rasmussen, S.O., Andersen, K.K., Svensson, A.M., Steffensen, J.P., Vinther, B.M., Clausen, H.B., Siggaard-Andersen, M.L., Johnsen, S.J., Larsen, L.B., Dahl-Jensen, D., Bigler, M., Röthlisberger, R., Fischer, H., Goto-Azuma, K., Hansson, M.E., Ruth, U., 2006. A new Greenland ice core chronology for the last glacial termination. J. Geophys. Res. 111, D6.
Reidy, L.M., 2001. Evidence of Environmental Change over the last 2000 years at Mountain Lake. In: The Northern San Francisco Peninsula, California [M.A. Thesis]. University of California at Berkeley, p. 108.
Reidy, L.M., 2013. Lake Sediments as Evidence of Natural and Human-Induced Environmental Change from California and Nevada [Ph.D. Thesis]. University of California, Berkeley, p. 99.
Reimer, P., Austin, W.E.N., Bard, E., Bayliss, A., Blackwell, P.G., Bronk Ramsey, C., Butzin, M., Cheng, H., Edwards, R.L., Friedrich, M., Grootes, P.M., Guilderson, T.P., Hajdas, I., Heaton, T.J., Hogg, A.G., Hughen, K., Kromer, b., Manning, S.W., Muscheler, R., Palmer, J.G., Pearson, C., van der Plicht, J., Reimer, R., Richards, D.A., Scott, E.M., Southon, J.R., Turney, C.S.M., Wacker, L., Adolphi, F., Büntgen, U., Capano, M., Fahrni, S., Fogtmann-Schulz, A., Friedrich, R., Miyake, F., Olsen, J., Reinig, F., Sakamoto, M., Sookdeo, A., Talamo, S., 2020. The IntCal20 Northern Hemisphere Radiocarbon Age Calibration Curve (0-55 Cal kBP): Radiocarbon.
Reimer, P.J., Bard, E., Bayliss, A., Beck, J.W., Blackwell, P.G., Bronk Ramsey, C., Buck, C.E., Cheng, H., Edwards, R.L., Freidrich, M., Grootes, P.M., Guilderson, T.P., Haflidason, H., Hajdas, I., Hatte, C., Heaton, T.J., Hoffmann, D.L., Hogg, A.G., Hughen, K.A., Kaiser, K.F., Kromer, B., Manning, S.W., Niu, M., Reimer, R.W., Richards, D.A., Scott, E.M., Southon, J.R., Staff, R.A., Turney, C.S.M., van der Plicht, J., 2013. IntCal13 and Marine13 radiocarbon age calibration curves 0-50,000 years cal BP. Radiocarbon 55 (4), 1869–1887.
Reinemann, S.A., Porinchu, D.F., Bloom, A.M., Mark, B.G., Box, J.E., 2009. A multiproxy paleolimnological reconstruction of Holocene climate conditions in the Great Basin, United States. Quat. Res. 72 (3), 347–358.
Rhodes, E.J., 2011. Optically Stimulated Luminescence Dating of Sediments over the Past 200,000 Years. Annu. Rev. Earth Planet Sci. 39 (1), 461–488.
Rodysill, J.R., Anderson, L., Cronin, T.M., Jones, M.C., Thompson, R.S., Wahl, D.B., Willard, D.A., Addison, J.A., Alder, J.R., Anderson, K.H., Anderson, L., Barron, J.A., Bernhardt, C.E., Hostetler, S.W., Kehrwald, N.M., Khan, N.S., Richey, J.N., Starratt, S.W., Strickland, L.E., Toomey, M.R., Treat, C.C., Wingard, G.L., 2018. A North American Hydroclimate Synthesis (NAHS) of the Common Era. Global Planet. Change 162, 175–198.
Rood, D.H., Burbank, D.W., Finkel, R.C., 2011. Chronology of glaciations in the Sierra Nevada, California, from ^{10}Be surface exposure dating. Quat. Sci. Rev. 30 (5–6), 646–661.
Sanchez-Cabeza, J.A., Ruiz-Fernández, A.C., 2012. 210Pb sediment radiochronology: An integrated formulation and classification of dating models. Geochem. Cosmochim. Acta 82, 183–200.
Sarna-Wojcicki, A.M., Lajoie, K.R., Meyer, C.E., Adam, D.P., Rieck, H.J., 1991. Tephrochronologic correlation of upper Neogene sediments along the Pacific margin, coterminous United States. In: Morrison, R.B. (Ed.), Quaternary Nonglacial Geology; Conterminous U.S.: Decade of North American Geology. Geological Society of America, Boulder, CO, pp. 117–139.
Sieh, K., Bursik, M., 1986. Most recent eruption of the Mono Craters, eastern central California. J. Geophys. Res. 91 (B12), 12,539–12,571.
Smith, S.J., 1989. Pollen and Microscopic Charcoal Analysis of a Sediment Core from Swamp Lake, Yosemite National Park, California [M.S. Thesis]. Northern Arizona University.
Smith, S.J., Anderson, R.S., 1992. Late Wisconsin paleoecologic record from Swamp Lake, Yosemite National Park. California: Quat. Res. 38, 91–102.
Smoot, J.P., Litwin, R.J., Bischoff, J.L., Lund, S.J., 2000. Sedimentary record of the 1872 earthquake and "Tsunami" at Owens Lake, southeast California. Sediment. Geol. 135, 241–254.
Starratt, S., 2009. Holocene climate on the Modoc Plateau, northern California, USA: the view from Medicine Lake. Hydrobiologia 631 (1), 197–211.
Starratt, S.W., Barron, J.A., Kneeshaw, T., Phillips, R.L., Bischoff, J.L., Lowenstern, J.B., Wanket, J.A., 2003. A Holocene record from Medicine Lake, Siskiyou County, California: Preliminary diatom, pollen, geochemical, and sedimentological data. In: Proc. 19th PACLIM Workshop, Technical Report 71 of the Interagency Ecological Program for the San Francisco Estuary.
Steponaitis, E., Andrews, A., McGee, D., Quade, J., Hsieh, Y.-T., Broecker, W.S., Shuman, B.N., Burns, S.J., Cheng, H., 2015. Mid-Holocene drying of the U.S. Great Basin recorded in Nevada speleothems. Quat. Sci. Rev. 127, 174–185.
Stine, S., 1990. Late Holocene fluctuations of Mono Lake, eastern California. Palaeogeogr. Palaeoclimatol. Palaeoecol. 78, 333–381.
Stine, S., 1994. Extreme and persistent drought in California and Patagonia during mediaeval time. Nature 369, 546–549.
Street, J.H., Anderson, R.S., Paytan, A., 2012. An organic geochemical record of Sierra Nevada climate since the LGM from Swamp Lake, Yosemite. Quat. Sci. Rev. 40, 89–106.
Street, J.H., Anderson, R.S., Rosenbauer, R.J., Paytan, A., 2013. n-Alkane evidence for the onset of wetter conditions in the Sierra Nevada, California (USA) at the mid-late Holocene transition, ~3.0 ka. Quat. Res. 79, 14–23.
Stuiver, M., 1978. Carbon-14 dating: A comparison of beta and ion counting. Science 202 (4370), 881–883.
Stuiver, M., Grootes, P.M., 2000. GISP2 Oxygen Isotope Ratios. Quat. Res. 53 (3), 277–284.
Stuiver, M., Polach, H.A., 1977. Reporting of ^{14}C data. Radiocarbon 19 (3), 355–363.
Stuiver, M., Suess, H.E., 1966. On the relationship between radiocarbon dates and true sample ages. Radiocarbon 8, 534–540.
Stuiver, M., Reimer, P.J., Bard, E., Beck, J.W., Burr, G.S., Hughen, K.A., Kromer, B., McCormac, G., van der Plicht, J., Spurk, M., 1998. IntCal98 radiocarbon age calibration, 24,000-0 cal BP. Radiocarbon 40 (3), 1041–1083.
Taylor, R.E., 2016. Radiocarbon Dating: Development of a Nobel Method, Radiocarbon and Climate Change, pp. 21–44.
Telford, R., Heegaard, E., Birks, H., 2004. All age–depth models are wrong: but how badly? Quat. Sci. Rev. 23 (1–2), 1–5.
Theissen, K.M., Hickson, T.A., Brundrett, A.L., Horns, S.E., Lachniet, M.S., 2019. A record of mid- and late Holocene paleohydroclimate from Lower Pahranagat Lake, southern Great Basin. Quat. Res. 1–13.
Thompson, R.S., 1992. Late Quaternary environments in Ruby Valley, Nevada. Quat. Res. 37, 1–15.
Thompson, R.S., Oviatt, C.G., Honke, J.S., McGeehin, J.P., 2016. Late Quaternary Changes in Lakes, Vegetation, and Climate in the Bonneville Basin Reconstructed from Sediment Cores from Great Salt Lake. Lake Bonneville - A Scientific Update: Developments in Earth Surface Processes, pp. 221–291.
Trachsel, M., Telford, R.J., 2017. All age-depth models are wrong, but are getting better. Holocene 27 (6), 860–869.
Trumbore, S.E., Sierra, C.A., Hicks Pries, C.E., 2016. Radiocarbon Nomenclature, Theory, Models, and Interpretation: Measuring Age, Determining Cycling Rates, and Tracing Source Pools. Radiocarbon and Climate Change 45–82.
Tunno, I., Mensing, S.A., 2017. The value of non-pollen palynomorphs in interpreting paleoecological change in the Great Basin (Nevada, USA). Quat. Res. 87 (3), 529–543.
Wahl, D., Starratt, S., Anderson, L., Kusler, J., Fuller, C., Addison, J., Wan, E., 2015. Holocene environmental changes inferred from biological and sedimentological proxies in a high elevation Great Basin lake in the northern Ruby Mountains, Nevada, USA. Quat. Int. 387, 87–98.
Walker, M., Johnsen, S., Rasmussen, S.O., Popp, T., Steffensen, J.-P., Gibbard, P., Hoek, W., Lowe, J., Andrews, J., Björck, S., Cwynar, L.C., Hughen, K., Kershaw, P., Kromer, B., Litt, T., Lowe, D.J., Nakagawa, T., Newnham, R., Schwander, J., 2009. Formal definition and dating of the GSSP (Global Stratotype Section and Point) for the base of the Holocene using the Greenland NGRIP ice core, and selected auxiliary records. J. Quat. Sci. 24 (1), 3–17.
Wang, Y.J., Cheng, H., Edwards, R.L., An, Z.S., Wu, J.Y., Shen, C.C., Dorale, J.A., 2001. A high-resolution absolute-dated late Pleistocene monsoon record from Hulu Cave, China. Science 294 (5550), 2345–2348.
Wanket, J.A., 2002. Late Quaternary Vegetation and Climate of the Klamath Mountains [Ph.D. Thesis]. University of California, Berkeley, p. 238.
West, G.J., 1989. Late Pleistocene/Holocene vegetation and climate. In: Basgall, M., Hildebrandt, W.R. (Eds.), Prehistory of the Sacramento River Canyon, Shasta County, California. Center for Archaeological Research, University of California, Davis, pp. 36–55.
West, G.J., 2004. A late Pleistocene-Holocene pollen record of vegetation change from Little Willow Lake, Lassen Volcanic National Park, California. In: Starratt, S.W., Blomquist, N.L. (Eds.), Twentieth Annual Pacific Climate Workshop: Pacific Grove, California, State of California. Dept. of Water Resources, pp. 65–80.
White, A., Briles, C., Whitlock, C., 2015. Postglacial vegetation and fire history of the

southern Cascade Range, Oregon. Quat. Res. 84 (3), 348–357.
Whitlock, C., Marlon, J., Briles, C., Brunelle, A., Long, C., Bartlein, P., 2008. Long-term relations among fire, fuel, and climate in the north-western US based on lake-sediment studies. Int. J. Wildland Fire 17, 72–83.
Wigand, P.E., 1987. Diamond Pond, Harney County, Oregon: Vegetation history and water table in the eastern Oregon desert. Great Basin Nat. 47 (3), 427–458.
Yang, I.C., 1988. US Geological Survey, Denver, Colorado Radiocarbon Dates V. Radiocarbon 30 (1), 41–60.
Yuan, F., Linsley, B.K., Howe, S.S., 2006a. Evaluating sedimentary geochemical lake-level tracers in Walker Lake, Nevada, over the last 200 years. J. Paleolimnol. 36 (1), 37–54.
Yuan, F., Linsley, B.K., Howe, S.S., Lund, S.P., McGeehin, J.P., 2006b. Late Holocene lake-level fluctuations in Walker Lake, Nevada, USA. Palaeogeogr. Palaeoclimatol. Palaeoecol. 240 (3–4), 497–507.
Yuan, F., Linsley, B.K., Lund, S.P., McGeehin, J.P., 2004. A 1200-year record of hydrologic variability in the Sierra Nevada from sediments in Walker Lake, Nevada. G-cubed 5 (3), 13.
Zimmerman, S.R.H., Hemming, S.R., Kent, D.V., Searle, S.Y., 2006. Revised chronology for late Pleistocene Mono Lake sediments based on paleointensity correlation to the global reference curve. Earth Planet Sci. Lett. 252, 94–106.
Zimmerman, S. R. H., Hemming, S. R., and Starratt, S. W., accepted, Holocene sedimentary architecture and paleoclimate variability at Mono Lake, CA, *in* Starratt, S. W., and Rosen, M. R., eds., From Saline to Freshwater: the Diversity of Western Lakes in Space and Time, Geological Society of America Special Paper 536.
Zimmerman, S.R.H., Brown, T.A., Hassel, C., Heck, J., 2018. Testing Pollen Sorted by Flow Cytometry as the Basis for High-Resolution Lacustrine Chronologies: Radiocarbon, pp. 1–16.